Title
Surface lesions of bone.

Journal
Radiology, 206(1)

ISSN
0033-8419

Authors
Seeger, LL
Yao, L
Eckardt, JJ

Publication Date
1998

DOI
10.1148/radiology.206.1.9423647

Peer reviewed

Leanne L. Seeger, MD
Lawrence Yao, MD
Jeffrey J. Eckardt, MD

Index terms:
Bone neoplasms, CT, 40.1211
Bone neoplasms, diagnosis, 40.31, 40.32
Bone neoplasms, secondary, 40.33
Bones, injuries, 40.41, 40.44
Bones, infection, 40.20, 40.352
Bones, radiography, 40.11
Fractures, 40.41
State-of-art reviews

Radiology 1998; 206:17–33

Abbreviation:
SE = spin echo

[1] From the Departments of Radiological Sciences (L.L.S., L.Y) and Orthopaedic Surgery (J.J.E.), UCLA School of Medicine, 200 Medical Plaza, Suite 165-59, Los Angeles, CA 90095-6952. Received June 25, 1997; revision requested July 21; revision received August 11; accepted August 15. **Address reprint requests to** L.L.S.

Surface Lesions of Bone[1]

A surface lesion of bone may arise within the cortex, between the cortex and the periosteum, within the periosteum, or in the tissues immediately adjacent to the periosteum including tendinous and ligamentous attachments. While these lesions generally reflect the spectrum of more common intramedullary lesions and have an appearance similar to that of their intramedullary counterparts, their unusual surface origin often renders diagnosis difficult. Surface sarcomas are usually of a lower grade than that of the intramedullary tumor, and often they have a more favorable prognosis. Traumatic lesions of the bone surface are common and should be considered in the differential diagnosis of a surface lesion, especially in the young or athletic individual. An elevated peripheral white blood cell count and erythrocyte sedimentation rate may herald an infection of the bone surface.

A surface lesion of bone refers to an entity that arises within or on a portion of the bone that is external to the medullary cavity. This includes tissues from the inner surface of the cortex to those external to the periosteum. Such lesions may be of neoplastic, traumatic, or infectious origin. This article discusses the imaging features of various surface lesions of bone, emphasizing techniques that assist in lesion characterization and management.

While some surface lesions have a classic appearance at imaging, many are nonspecific. Correlation with clinical information including history (presence, duration, and pattern of pain) and laboratory values (peripheral white blood cell count and erythrocyte sedimentation rate) are often key to the appropriate diagnosis. As with intramedullary tumors, differentiation between a benign lesion and its low-grade, malignant counterpart is generally impossible with imaging alone, and biopsy is essential to establish a diagnosis and to direct management.

While the discussion is intended to be broad, it is not all inclusive. Extremely rare surface lesions have been intentionally omitted. Discussion of generalized periosteal abnormalities arising from systemic or metabolic disorders is beyond the scope of this article.

TERMINOLOGY

Surface lesions are designated according to the location of origin within or on the surface of a bone. This terminology can be confusing or invalid, as the exact site of origin may not be evident either radiographically or histologically. For this reason, descriptive terms are often intentionally vague.

The bone surface includes three distinct regions: the cortex, the periosteum, and the fibrous tissues immediately superficial to the periosteum. An *endosteal* lesion is one that originates within the inner cortex of the bone, adjacent to the medullary cavity. An *intracortical* lesion is centered within the cortex. A *subperiosteal* process begins immediately beneath the periosteum (between the cortex and periosteum), and a *periosteal* lesion originates within the periosteum. The terms *parosteal* and *juxtacortical* are synonymous. These more general descriptors refer to the fibroblastic tissues external to the cortex, including the periosteum and adjacent ligaments, tendons, and fascia. Many authors further interchange the terms *parosteal* and *juxtacortical* with *periosteal*. A periosteal origin is probably best considered a separate entity. This is especially true in the case of parosteal and periosteal osteosarcoma, as these two tumors represent histologically distinct processes. When the site of origin of a lesion within the surface of a bone cannot be determined or is variable, the term *paracortical* is appropriate. This includes all tissues from the endosteum to the periosteum.

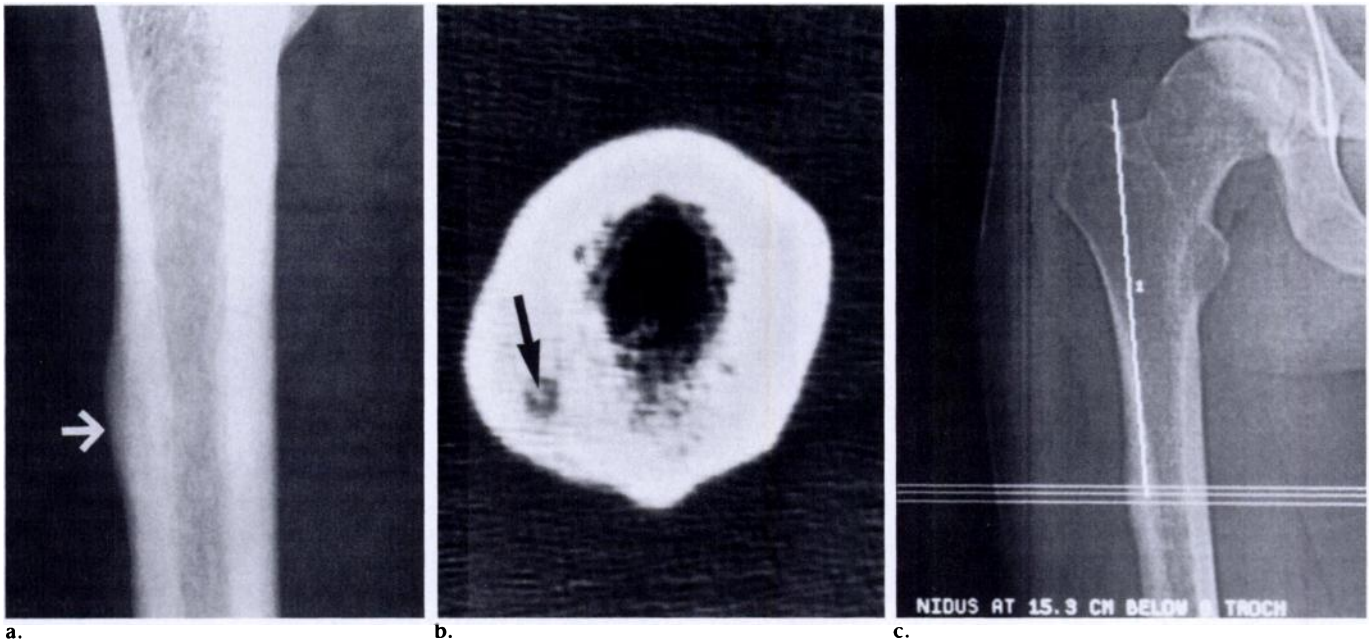

a. b. c.

Figure 1. Osteoid osteoma. **(a)** Anteroposterior radiograph of the femur shows fusiform, benign-appearing cortical thickening of the lateral aspect of the proximal femoral shaft (arrow). A nidus is not evident. **(b)** Thin-section (3-mm) computed tomographic (CT) image. The intracortical nidus is evident posterolaterally, at approximately the 7-o'clock position (arrow). **(c)** Measurements for intraoperative planning. The level of the nidus is located on the scout image. A measurement is made from the top of the greater trochanter (a surgically palpable landmark) to the level of the nidus. In this case, the distance measures 15.3 cm.

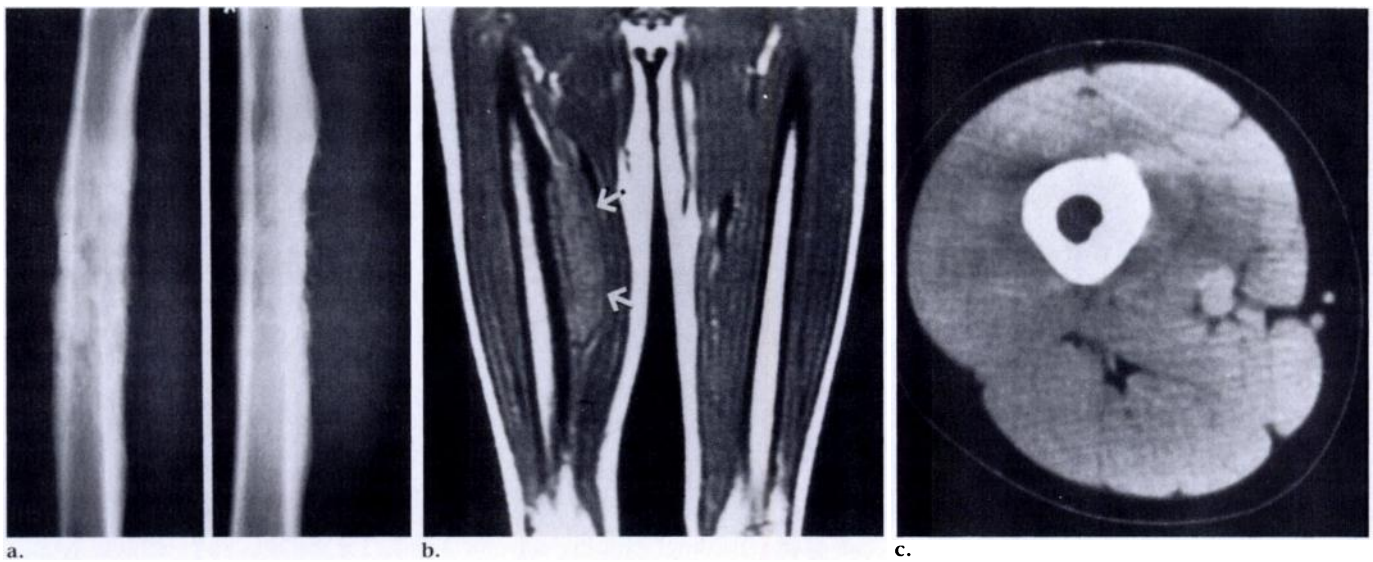

a. b. c.

Figure 2. Parosteal Ewing sarcoma. **(a)** Lateral and anteroposterior radiographs of the femoral shaft reveal cortical thickening, which is associated with surface scalloping and irregular perpendicular spicules of periosteal new bone. **(b)** Coronal T1-weighted magnetic resonance (MR) image (spin echo [SE]; repetition time msec/echo time msec, 500/20) shows the lesion (arrows) to arise on the surface of the medial cortex. The underlying medullary cavity is normal. **(c)** Contrast material–enhanced CT image. The findings confirm the absence of medullary involvement. The soft-tissue mass, however, is much better appreciated on the MR image.

ORIGIN

A primary surface lesion of bone may arise from any of the mesenchymal elements that normally reside there, or it may be the product of the pluripotential cells of the parosteal tissues. Thus, a surface lesion may contain osteoid, cartilage, fibrous tissue, fat, or blood vessels. Secondary surface lesions refer to paracortical metastatic disease and will have a cell type that reflects that of the primary tumor.

As with primary intramedullary bone tumors, benign neoplastic surface lesions have malignant (sarcomatous) counterparts. Surface sarcomas generally have a more favorable prognosis than a histologically identical intramedullary lesion.

Traumatic surface lesions may be composed of the same tissue types as true neoplasia. These masses often contain anaplastic cells and a relatively high number of mitotic figures, which renders histologic differentiation from malignancy

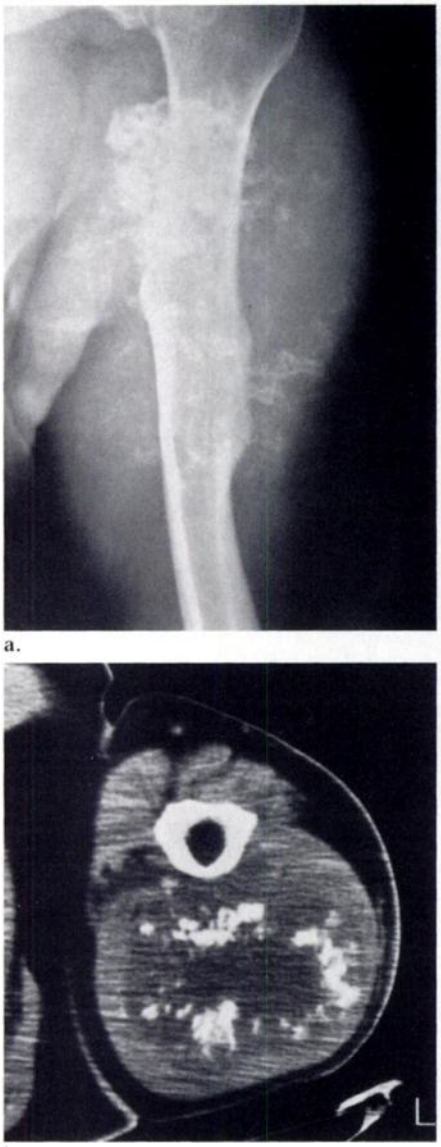

Figure 3. Parosteal chondrosarcoma. **(a)** Anteroposterior radiograph of the humerus reveals a large soft-tissue mass associated with the midshaft to proximal shaft. Extensive matrix mineralization is present, including circular calcifications that indicate a cartilage component. **(b)** CT image shows the lesion to arrive from the posterior cortex of the humeral shaft. There is no medullary involvement. The tumor is of lower attenuation than the surrounding muscles, suggesting a chondroid origin.

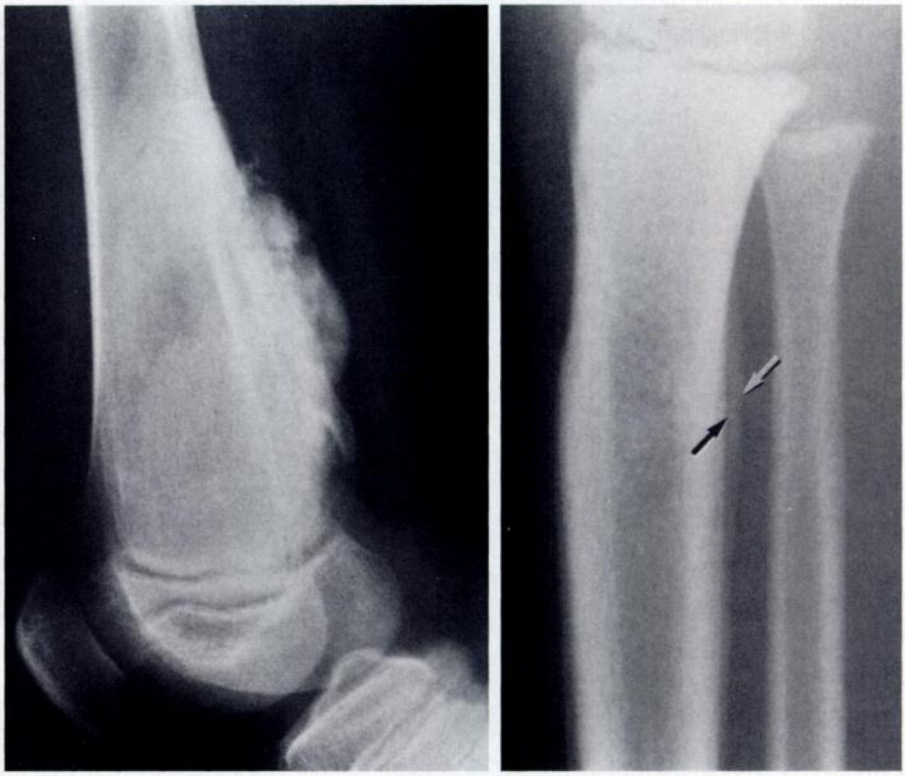

Figures 4, 5. **(4)** Parosteal osteosarcoma. Lateral radiograph of the distal femur shows a heavily mineralized lesion associated with the surface of the posterior femoral shaft. **(5)** Stress fracture. Lateral radiograph reveals benign-appearing periosteal new bone along the posterior tibia. A subtle fracture line is evident (arrows).

challenging even to the experienced pathologist. A thorough clinical history and correlation with imaging are often necessary in establishing a benign traumatic origin.

Infections of the bone surface may result from contiguous spread from the medullary cavity, direct inoculation, or hematogenous spread.

A small number of benign processes that may affect the surface of a single bone are of unknown origin. While some of these lesions have a typical histologic appearance, the imaging and histologic appearances are often nonspecific and diagnosis is one of exclusion.

GENERAL IMAGING PRINCIPLES

Imaging evaluation of a bone lesion should begin with plain radiography in at least two perpendicular planes. This will usually be sufficient to determine if a lesion originates in the soft tissues, within the medullary cavity, or on the surface of the bone. Occasionally, oblique views (under fluoroscopic guidance as needed) may assist in confirming a surface origin.

Once a lesion is detected, further evaluation will be guided by the working differential diagnosis. Careful radiographic analysis should determine if a lesion is likely benign and slow growing or aggressive. The nature of periosteal new bone must be scrutinized. Uniform, uninterrupted, uni- or multilaminar periosteal new bone is a fairly reliable indication of benignity (Fig 1a). Malignant periosteal reactions are more often interrupted and may contain perpendicular bone spicules (Fig 2a). The Codman triangle, an abrupt cutoff of periosteal new bone at the edge of the lesion, represents a mass elevating the periosteum. Although the Codman triangle is generally associated with malignancy, this feature may also be seen with a number of aggressive benign conditions.

Plain radiographic evaluation should also be used to assess the margins and internal composition of the lesion. Well-defined margins suggest benignity, while permeative margins indicate an aggressive process. One should decide if the lesion is purely lytic or if there is matrix mineralization. Cartilage matrix mineralization usually appears as well-defined, punctate opacities that often form circles or incomplete rings (Fig 3a). Osteoid mineralization is more amorphous and cloudlike (Fig 4).

If the lesion appears benign radiographically and surgical intervention is not contemplated, no further imaging is needed. This would be the case in, for example, a stress fracture in which benign-appearing periosteal new bone is

maturing and the fracture line can be seen on the radiographs (Fig 5). If the origin of the abnormality is unclear radiographically, cross-sectional imaging can assist in characterizing the origin, location, and extent of the lesion. In general, CT is preferred for this purpose because it has a superior ability to depict focal areas of osteolysis or matrix mineralization and subtle cortical abnormalities. CT should be performed with a bone algorithm and a field of view as small as possible to permit visualization of the entire lesion. Thin-section imaging should be used for small lesions.

MR imaging is usually superior to CT for demonstrating any associated soft-tissue mass (Fig 2b, 2c) and is therefore useful for preoperative planning once a diagnosis is established. Imaging with a surface coil is usually desirable for enhanced resolution.

Radionuclide bone scanning is useful primarily for excluding multifocal bone involvement. Bone scanning may also be useful for gauging the metabolic activity of a lesion that is thought to be benign; normal tracer accumulation indicates that a radiographically benign-appearing lesion can be followed clinically. Routine use of radionuclide imaging is not indicated and usually will not narrow the differential diagnosis.

Ultrasound (US) may be useful for documenting the fluid nature of such lesions as parosteal abscess or ganglion, but generally it cannot be used to establish a diagnosis.

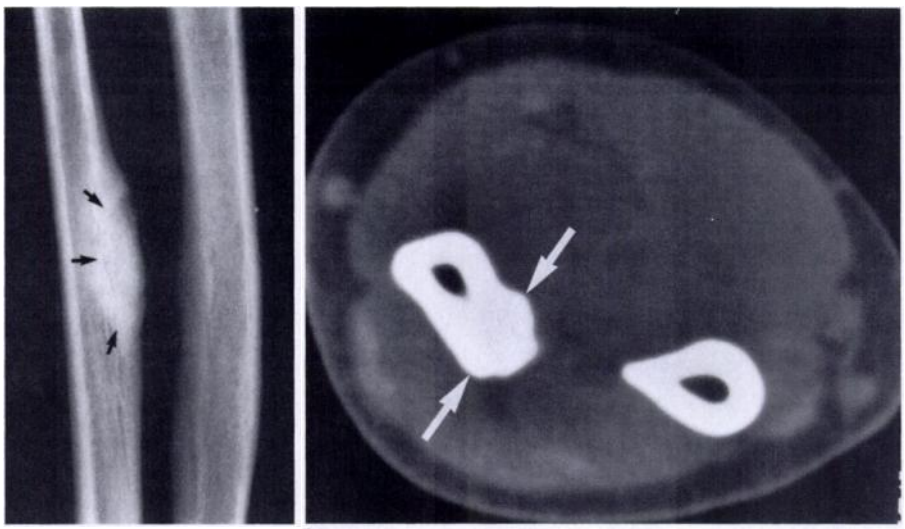

Figure 6. Osteoma of long bone. **(a)** Posteroanterior radiograph of the midforearm shows a dense lesion (arrows) involving the cortex of the ulna. **(b)** Axial CT image. The lesion (arrows) is of uniform attenuation. The medullary cavity is not involved.

BONE-FORMING TUMORS

Benign bone-forming lesions that may arise in or on the surface of a bone include osteoma, osteoid osteoma, and osteoblastoma. Their malignant counterparts are variations of the surface osteosarcoma, including parosteal, periosteal, and high-grade surface osteosarcoma. For diagnostic purposes, plain radiography may suffice for the imaging evaluation of a bone-forming neoplasia if matrix mineralization is evident. In cases in which additional characterization is needed, CT is generally superior to MR imaging. CT will best define thin lines of sclerosis surrounding a lesion, subtle cortical defects or erosion, and intralesional mineralization.

Osteoma

Osteomas most frequently occur in the craniofacial bones and the mandible. While multifocal osteomas may be seen in Gardner syndrome (1), a solitary lesion does not indicate an underlying generalized disorder. Solitary appendicular osteomas are rare.

The osteoma is a juxtacortical lesion. It may be distinguished from the intramedullary bone island (enostosis) not only on the basis of location but also on the basis of histologic characteristics. A bone island is composed of compact lamellar bone and contains Haversian systems. An osteoma is usually a mixture of lamellar and woven bone, with or without Haversian systems (2). When an osteoma is composed primarily of compact bone, it will appear radiographically as a contour deformity of the cortex that blends with the surrounding cortical bone (Fig 6). When composed primarily of trabecular bone and marrow, the interface between the osteoma and adjacent bone will be more distinct. Once the lesion is detected radiographically, CT is useful for confirming the homogeneous attenuation of the lesion and a location that is confined to the bone cortex (3).

Differentiation of an osteoma from a parosteal osteosarcoma can be difficult both radiographically and histologically, and detailed tissue analysis is needed in all cases. The diagnosis of a parosteal osteosarcoma is suggested by the presence of spindle cell proliferation on a biopsy sample (4), but this finding may be missed if the sample is relatively small. Consequently, some authors recommend surgical excision with wide margins to allow complete histologic evaluation (5). Others, however, believe that it is safe to follow suspected osteomas of long bones clinically and radiographically if the diagnosis of osteoma is made on the basis of findings from the initial biopsy (3).

Osteoid Osteoma

Although some investigators have suggested that osteoid osteoma is a posttraumatic (6) or inflammatory (7) process, most authors now think that this lesion represents benign neoplasia (8). Surface osteoid osteomas may arise either within the cortex (including the endosteal surface) or in a subperiosteal or intraperiosteal location. The patient generally complains of intense pain that is most severe at night. Pain relief can usually be achieved with nonsteroidal anti-inflammatory medications. Very rare conditions of multicentric (9) or multifocal (10) osteoid osteoma have been described.

The lesion itself (the nidus) is round to oval and usually measures less than 1 cm in diameter. The nidus of the osteoid osteoma is usually a radiolucent focus but may be calcified to a varying degree. When sclerotic, the nidus is surrounded by a thin rim of radiolucency representing a peripheral fibrovascular zone (Fig 1b) (11).

The cortical osteoid osteoma is the most common. When the lesion occurs in the diaphysis or metaphysis of a bone, it is surrounded by uninterrupted, fusiform, benign-appearing reactive sclerosis that represents both cortical and periosteal reaction (Fig 1a) (12). Lesions at the end of a bone may appear lytic with little

or no surrounding sclerosis (13). This is due to the inability of intracapsular periosteum to produce proliferative, sclerotic new bone (8,14).

Plain radiographs are diagnostic of osteoid osteoma if the nidus can be identified. When the nidus cannot be seen on radiographs, the differential diagnosis includes other lesions that can be associated with intense, benign-appearing new bone formation, including stress fracture, eosinophilic granuloma, and infection. Radionuclide imaging and MR imaging generally do not assist in differentiating these processes; all will be associated with intense tracer uptake on the bone scan, and all will usually show surrounding marrow and soft-tissue edema at MR imaging (15). In addition, the nidus may easily be overlooked with MR imaging (16,17). Thin-section CT is best suited to depict the nidus (Fig 1b).

The scout CT image should include the entire bone in question, and thin-section cuts should be restricted to the area of sclerosis. The report should identify the location of the lesion around the circumference of the bone, as on the face of a clock. Measurements made on the scout image from the center of the nidus to palpable surgical landmarks (Fig 1c) are of great assistance to the surgeon and ensure targeted excision of the nidus that preserves the surrounding reactive bone.

Because the nidus is typically small, surgical localization of the lesion can be challenging. Intraoperative localization with bone scintigraphy has been used in the past (18), but this method can be cumbersome in the operating room. Preoperative CT-guided placement of a wire within the nidus has also been suggested (19), as has CT-guided boring of the overlying cortex with a needle dipped in methylene blue (20). These procedures are not necessary if accurate preoperative CT measurements are made.

Treatment of osteoid osteoma is rapidly evolving and controversial. The pain can be controlled with anti-inflammatory medication in most individuals, and resolution of symptoms and the nidus has been documented (21). Some authors, therefore, advocate long-term medical treatment until symptoms remit. For patients who cannot tolerate long-term anti-inflammatory treatment, the nidus should be excised. While this has traditionally been done in the operating room at open excision, several reports have demonstrated successful ablation of the nidus by using CT-guided percutaneous drilling and/or excision (22–24). More recently, percutaneous radio-frequency ablation of osteoid osteomas has been reported (25).

Paracortical Osteoblastoma

Osteoblastoma is differentiated from osteoid osteoma on the basis of the tumor size (larger than 2 cm) and a lack of response to nonsteroidal anti-inflammatory medications. Some authors argue that there are also subtle histologic differences between these two lesions (26). Although osteoblastomas are usually intramedullary lesions, an intracortical location is not uncommon. In one report of 98 cases of osteoblastoma, 42% were thought to arise in the cortex (27). Because of their large size and frequent location on the spine, osteoblastomas are more likely to be associated with neurologic symptoms than are osteoid osteomas (28). Multiple osteoblastoma-like lesions in one lower extremity have been reported, representing both intramedullary and intracortical lesions (29).

The surface osteoblastoma appears similar to its intramedullary counterpart. The lesion is round to oval in shape, well defined, and usually surrounded by a thin sclerotic rim. It may be radiolucent or may contain matrix mineralization. CT is the preferred modality for cross-sectional evaluation, as it will show the border and lesion mineralization. MR imaging findings can be confusing, especially in cases of so-called aggressive osteoblastoma. These lesions are associated with intense bone and soft-tissue edema that may mask the tumor or cause gross overestimation of the size of the lesion (30).

Surface Osteosarcoma

Surface osteosarcomas have conventionally been divided into three subtypes: parosteal, periosteal, and high-grade surface (31). A fourth variety, the cortical osteosarcoma, has also been well described (32,33). Distinction into these categories addresses the prognosis and affects treatment. Classification is possible with careful histologic analysis.

The parosteal osteosarcoma (Fig 4) is the most common of the surface osteosarcomas. The lesion is usually metaphyseal and frequently located along the posterior aspect of the distal femoral shaft, and it should not be confused with an osteochondroma. The tumor is usually densely mineralized, in either an amorphous, uniform, striated, or lobulated fashion (34). When large, the tumor may encircle the bone. The importance of intramedullary involvement by parosteal osteosarcoma is debated. Some authors believe that this finding is associated with a poorer outcome (31), while others believe that medullary invasion is not a prognostic indicator (34,35). Although the tumor is usually low grade, differentiation to a high-grade sarcoma is not uncommon and is associated with an increased incidence of metastatic disease and a poorer outcome (36).

Periosteal osteosarcoma is far less common than the parosteal variety. The prognosis for the periosteal osteosarcoma is worse than that for the parosteal tumor but better than for the high-grade surface osteosarcoma. The periosteal osteosarcoma is often diaphyseal and frequently found on the tibia. Some authors think that a femoral location is associated with a less favorable outcome than a tibial lesion, perhaps because the tumor is not discovered until it has reached a larger size (37). Femoral periosteal osteosarcoma is usually located in the anterior, lateral, or medial portion of the bone. Regardless of location, the underlying cortex may be thickened, and spicules of perpendicular bone may radiate into the adjacent soft-tissue mass (31). Histologically, the tumor is chondroblastic and usually of moderate grade.

As implied in the name, the high-grade surface osteosarcoma carries a prognosis less favorable than the parosteal or periosteal surface lesions. Histologically, the lesion is identical to the conventional high-grade intramedullary lesion. Radiographically, the tumor is broad based and abuts the adjacent cortex (31). The mass may be lightly or heavily mineralized.

The intracortical osteosarcoma is also a high-grade lesion and thus histologically similar to the conventional intramedullary osteosarcoma. Whereas the high-grade surface variety arises superficial to the cortex of the bone, the intracortical lesion arises within the cortex. While most reported cases have been confined within the cortex, a large soft-tissue mass may be present (33).

CARTILAGE-FORMING TUMORS

Cartilaginous surface lesions represent either an extension of a lesion contiguous with the medullary cavity or the counterpart of a more common, histologically identical or similar intramedullary lesion. At both MR imaging and CT, cartilaginous lesions often have a lobulated appearance that will assist in determining the tissue of origin. CT is usually preferred, as classic cartilage mineraliza-

tion will be overlooked on MR images. Lesion attenuation lower than that of muscle on CT scans is also a clue to a cartilaginous lesion.

Osteochondroma

The solitary osteochondroma is a relatively common benign lesion. Although several theories about its origin have been proposed, some authors believe that the lesion is a result of a defect in the periosteal bone surrounding the epiphyseal plate in conjunction with separation of a piece of the physeal cartilage (38). With skeletal growth, the lesion is transported along the length of the bone until it reaches a metaphyseal or diaphyseal location. The younger the patient, the closer the lesion will be to the growth plate. The lesion generally ceases to grow at the time of skeletal maturity. The osteochondroma has classic imaging features, including continuity of the marrow and cortex of the lesion with that of the parent bone (Fig 7). It may have either a broad sessile base or a pedunculated stalk.

The osteochondroma can usually be diagnosed with plain radiography alone. If the lesion is asymptomatic, it can be followed radiographically and clinically until cessation of growth. A benign osteochondroma may become painful for a number of reasons, including fracture through the stalk, development of an overlying bursa, or compression of adjacent neurovascular structures. If an osteochondroma suddenly becomes painful or grows after skeletal maturity, malignant transformation to chondrosarcoma should be suspected. The sarcomatous lesion arises in the chondroid cells of the cap, and a cartilage cap more than 2–3 cm thick is an indication of possible malignancy (Fig 8). This feature is easily demonstrated with cross-sectional imaging. With MR imaging, the cap will have low signal intensity on T1-weighted images and high signal intensity on T2-weighted images. Although secondary chondrosarcomas are usually low grade and can be treated with wide resection alone, dedifferentiation into a higher grade sarcoma (osteosarcoma or fibrosarcoma) can occur (39,40).

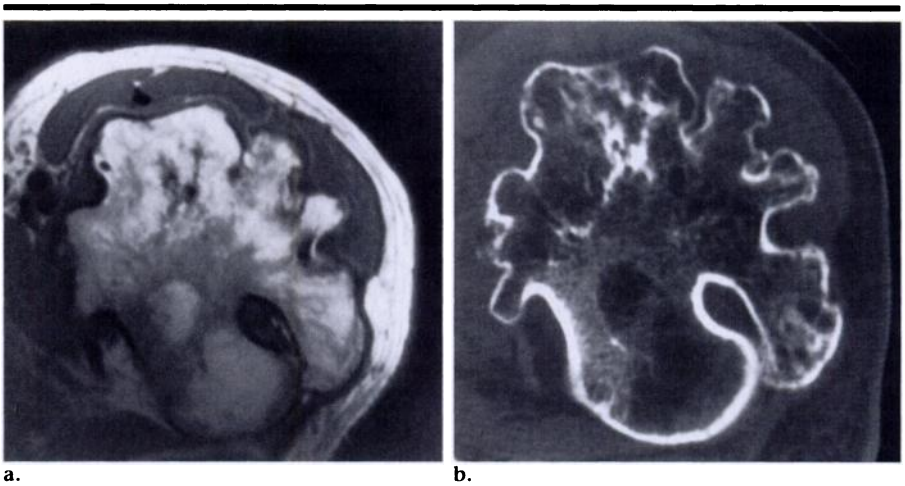

a. b.

Figure 7. Osteochondroma. **(a)** Axial T1-weighted MR image (SE 700/11). **(b)** CT image. Both the MR and the CT images show that the lesion is contiguous with the medullary cavity of the proximal femur and contains normal-appearing trabeculae and fat. The cartilage cap is very thin and difficult to see with either modality.

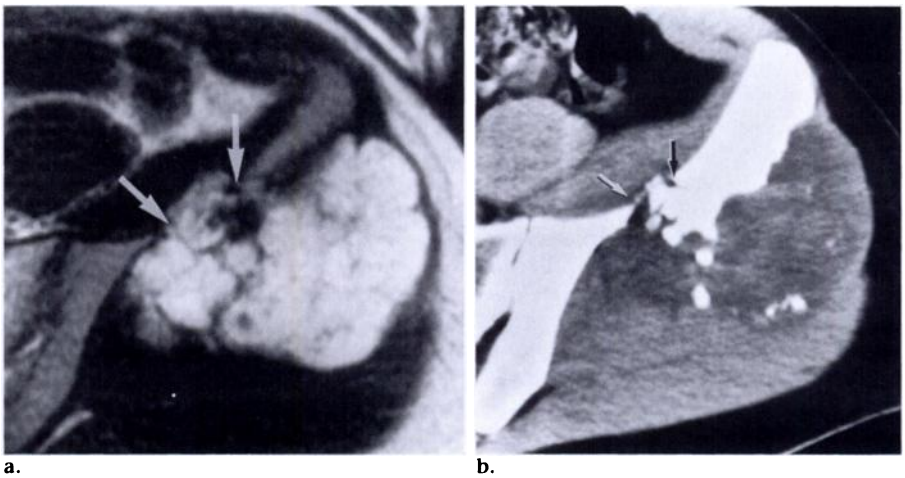

a. b.

Figure 8. Secondary chondrosarcoma arising in osteochondroma. **(a)** Axial T2-weighted MR image (SE 1,800/70). **(b)** CT image obtained with soft-tissue window. Both the MR and the CT images demonstrate the destruction of the medial aspect of the iliac wing (arrows). The lobulated nature of the mass suggests a chondroid origin. The relative low attenuation of the mass and the calcifications on the CT scan are typical of a cartilage lesion.

Juxtacortical (Periosteal) Chondroma

The juxtacortical chondroma represents the surface variant of an enchondroma. This is a lesion of children and young adults. The long bones are commonly affected, and there is a peculiar propensity for the lesion to be located in the proximal humerus (Fig 9) (41). Some authors have implicated a traumatic origin (42). There are no reports of malignant transformation of a parosteal chondroma (43).

As with the enchondroma, the surface chondroma may be purely lytic or may show internal chondroid mineralization. The adjacent cortex may be normal, smoothly saucerized and sclerotic, or focally destroyed. If associated with a substantial soft-tissue extension, a thin shell of periosteal new bone may surround the exterior of the lesion (44). When multiple lesions are present, consideration should be given to the diagnosis of Ollier disease.

Paracortical Chondromyxoid Fibroma

Chondromyxoid fibroma is the least common of the benign tumors of chondroid origin. The surface variety is distinctly rare; to our knowledge, only 10 cases have been reported in the English-language literature (45). Both the medullary and cortical chondromyxoid fibromas usually involve the metaphysis of a long bone. The lesion generally appears on radiographs as a well-defined radiolucent focus that is either round or oval.

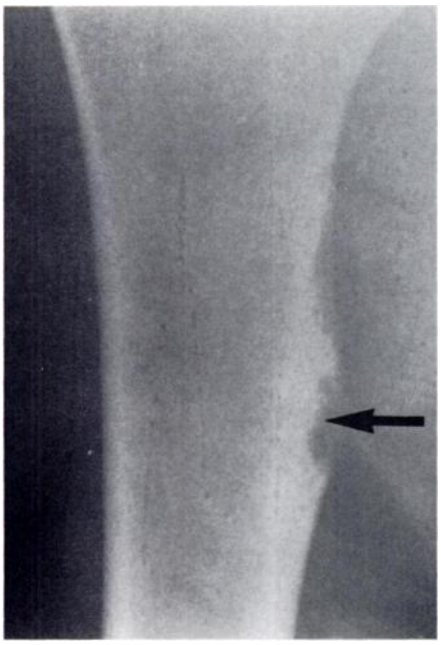

Figure 9. Juxtacortical chondroma. Anteroposterior radiograph of the proximal humerus shows benign-appearing cortical thickening with a central elongated radiolucency (arrow).

Typical chondroid mineralization is usually lacking (46), which renders the diagnosis difficult on the basis of imaging findings alone. Histologically, the lesion is multinodular and composed of a mixture of chondroid, myxoid, and fibrous tissue. Focal hypercellularity and unusual cytoplasmic and nuclear shapes may lead to an erroneous diagnosis of chondrosarcoma (47).

Bizarre Parosteal Osteochondromatous Proliferation

This rare entity, also know as a Nora lesion, usually manifests as a painless mass. The origin is debated. Some believe that the lesion is posttraumatic (48), while others favor a neoplastic origin on the basis of frequent recurrence following resection (49). Bizarre parosteal osteochondromatous proliferation is most commonly found along the small bones of the hands and feet, but it has also been reported to involve the skull and the long bones of the upper and lower extremities (49).

Early on, the lesion appears as an immature mass of mineralization within the soft tissues with no clear osseous attachment (49). When mature, the lesion is adherent to the adjacent bone with a pedunculated or sessile base. Radiographically, it may simulate an osteochondroma. This diagnosis can be excluded by the lack of marrow and cortical continuity with the underlying bone.

Parosteal Chondrosarcoma

The parosteal chondrosarcoma is a controversial lesion. Differentiation of parosteal chondrosarcoma from the more common periosteal osteosarcoma is debated (50–53). Some believe that these two lesions may coexist (54), rendering classification into a distinct category difficult. Just as the origin of the lesion is poorly understood, the radiographic appearance is variable. The tumor may be metaphyseal to diaphyseal, and round to lobulated. It may or may not contain intralesional mineralization (Fig 3). The underlying cortex may be essentially normal, thickened, or eroded and saucerized. In contradistinction to periosteal osteosarcoma, perpendicular or radial periosteal new bone formation is lacking. Lymph node metastasis has been reported, and the tumor may be present for many years prior to diagnosis (50).

Plain radiographs will generally be unrewarding when the underlying cortex is normal and the tumor is not mineralized. Either MR or CT will display the soft-tissue mass and confirm the lack of medullary involvement. CT is preferred for the demonstration of intralesional mineralization.

FIBROUS TUMORS

Benign fibrous lesions of the bone surface are common, but their malignant counterparts are extremely rare. Lacking mineralization, these lesions will appear as radiolucent defects on plain radiographs. The role of cross-sectional imaging is generally to define the extent of a known lesion. Early reports suggested that fibrous lesions showed a typical appearance of low signal intensity on T2-weighted MR images (55). Unfortunately, many fibrous lesions with a classic radiographic appearance have a variable MR appearance (56).

Fibrous Cortical Defect and Nonossifying Fibroma

The fibrous cortical defect represents a benign intracortical or rarely juxtacortical focus of fibrous tissue. These lesions are extremely common; Caffey (57) has determined that up to 36% of children will develop one or more of these lesions. The radiographic appearance of a fibrous cortical defect is classic. The lesion begins in a metaphyseal location but may extend into the diaphysis with skeletal growth. It usually begins as an oblong radiolucent focus. With time, a well-defined border of sclerosis will develop. In most instances, the lesion will regress, filling in with bone from the periphery to the center. Eventually, the lesion cannot be seen radiographically.

While this is the usual course of events, a fibrous cortical defect may continue to grow and involve the medullary portion of the bone. Once this has occurred, the lesion is termed a nonossifying fibroma (fibroxanthoma) (Fig 10). On radiographs, this lesion is radiolucent and multiloculated and has a well-defined sclerotic border. The term nonossifying fibroma is actually a misnomer, as the lesion will eventually ossify and regress in a manner similar to the typical fibrous cortical defect (Fig 11). If the lesion has become large, benign-appearing bone expansion may persist into adult life even after the lesion itself has involuted. The condition of multiple nonossifying fibromas in conjunction with café-au-lait spots of varying size and configuration has been termed Jaffe-Campanacci syndrome (58).

The need for further imaging evaluation and treatment of a nonossifying fibroma will be determined on the basis of the size and location of the lesion. When the lesion is an incidental finding and relatively small, no further imaging is warranted as long as the patient remains asymptomatic. Some would advocate serial radiographic assessment to ensure that the lesion does not grow. If a lesion with a typical radiographic appearance of fibrous cortical defect or nonossifying fibroma becomes painful, it has probably undergone microfracture that may not be radiographically evident. These lesions should be treated with curettage and bone grafting. Large nonossifying fibromas at risk of pathologic fracture should be curetted and packed with bone graft. When surgical intervention is planned, CT is warranted to define the extent of intramedullary involvement and assist in determining the surgical approach.

Juxtacortical Desmoplastic Fibroma (Desmoid Tumor)

Also known as aggressive fibromatosis, this low-grade neoplastic lesion has histologic features that are indistinguishable from those of intramedullary or soft-tissue desmoid tumors. This true desmoid tumor is to be distinguished from the cortical irregularity syndrome of the dis-

tal femur (see below), which is of a traumatic origin. Histologically, differentiation of a surface desmoid from the extremely rare surface fibrosarcoma may be difficult.

When a desmoid tumor originates on or near the surface of a bone, it can extend into the soft tissues (Fig 12) and invade the adjacent bone causing erosion and saucerization. The presence of periosteal new bone formation usually implies the presence of a fracture (59).

Desmoplastic fibroma requires surgical intervention. Because the neoplasm is low grade, amputation or radical resection is not needed. Adequate surgical margins should, however, be obtained, as the risk for recurrent disease is high with inadequate excision (60). When adequate margins cannot be obtained, postoperative radiation therapy is probably indicated. Because the tumor may be associated with a substantial soft-tissue mass, MR imaging may be preferable for preoperative planning. Either MR or CT will adequately show the bone involvement.

Osteofibrous Dysplasia

Osteofibrous dysplasia (extragnathic ossifying fibroma) is a lesion of childhood that most commonly begins in the anterior cortex of the middle or distal third of the tibial diaphysis. The lesion may also be found in the fibula or in both bones simultaneously. The patient usually presents with local pain and/or swelling, or pathologic fracture. Radiographically, smooth or lobulated cortical expansion is seen (Fig 13), and the bone is often bowed anteriorly. The relatively radiolucent lesion is often surrounded by bone sclerosis (61).

The disease course of osteofibrous dysplasia is variable. Some lesions remain small and eventually regress, while others may lead to bowing of the bone or pathologic fracture. Treatment is quite controversial. Some authors have recommended that the lesion be resected en block and grafted. The experience of others suggests that a small and uncomplicated lesion is best followed clinically because the lesion will cease to grow after skeletal maturation (62).

Even more controversial is the possible relationship between osteofibrous dysplasia and adamantinoma, an epithelioid tumor of adulthood that may metastasize and kill the patient. Careful analysis of recurrent osteofibrous dysplasia may reveal foci of adamantinoma (63), leading some to consider osteofibrous dysplasia a "juvenile" form of this more aggressive tumor. Radiographically, osteofibrous dysplasia and adamantinoma may appear identical (61). Although the adamantinoma is generally considered to represent neoplasia, a history of trauma has been reported in up to 62% of patients with this lesion (64).

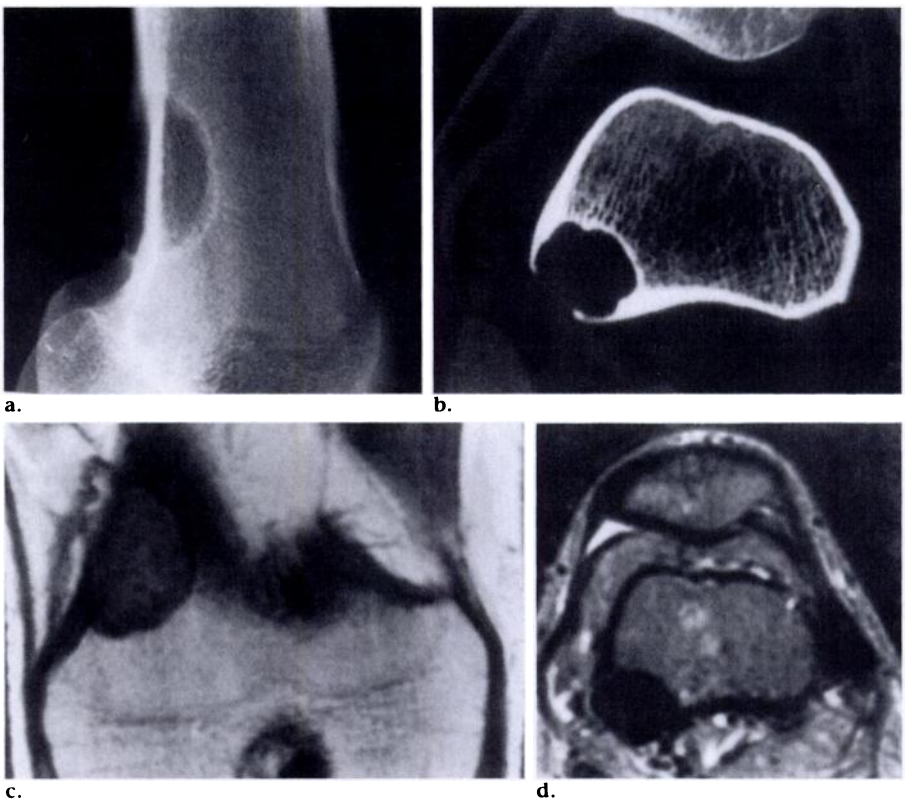

Figure 10. Nonossifying fibroma. **(a)** Lateral radiograph of the knee shows a 3.5-cm-long lesion involving the posterior femur. The lesion is well circumscribed and has a sclerotic margin. **(b)** Axial CT image. The lesion has breached the cortex. This is not an unusual finding and should not raise the suspicion of malignancy. **(c)** Coronal T1-weighted MR image (SE 500/30). **(d)** Axial T2-weighted MR image (SE 2,000/80). As would be expected for a bland fibrous lesion, this nonossifying fibroma has low signal intensity on both T1- and T2-weighted images. The cortical destruction seen on the CT scan is not evident on the MR images.

FATTY TUMORS

While most soft-tissue masses either are not evident on radiographs or show a tissue density equal to that of surrounding muscle, lesions with a high fat content are often well depicted. Both CT and MR imaging can demonstrate the presence of fat in a lesion; however, CT is preferable for documentation of any calcification that may be present.

Parosteal Lipoma

The origin of this unusual tumor is debated, but most believe that it arises from the tissues immediately superficial to the periosteum (65). The parosteal li-

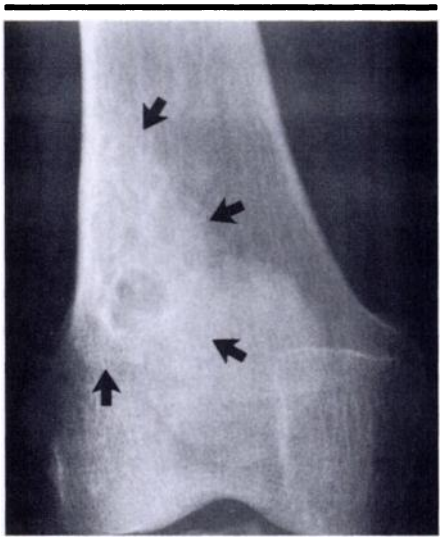

Figure 11. Involuting nonossifying fibroma. Radiograph shows a sclerotic lesion is present in the lateral aspect of the distal femur (arrows). This is associated with very subtle expansion of the distal shaft. The residual lucency appears slightly lobulated and has well-defined sclerotic borders.

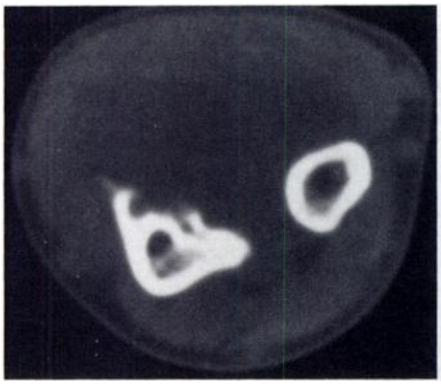

a.

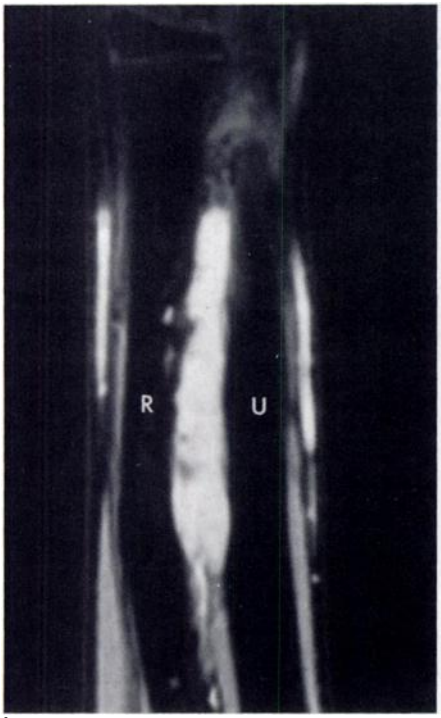

b.

Figure 12. Juxtacortical desmoplastic fibroma. **(a)** CT image shows a lesion that originates in the cortex of the radial shaft. **(b)** Multiplanar gradient-echo MR image obtained with spectral fat saturation (400/9, 30). The soft-tissue mass is well displayed. *R* = radius, *U* = ulna.

poma often manifests as a painless mass. When found in a relatively restricted compartment such as the forearm, the lesion may be associated with nerve compression (66).

Four appearances of parosteal lipoma have been described (67). Rarely, the lesion may be totally radiolucent. Most commonly, a pedunculated exostosis will be evident, surrounded by a radiolucent (fatty) cap (Fig 14). This may appear as subtle cortical thickening or may consist of a relatively large bone excrescence off the cortex (68). An osteochondromatous sessile lesion may also be seen, as may

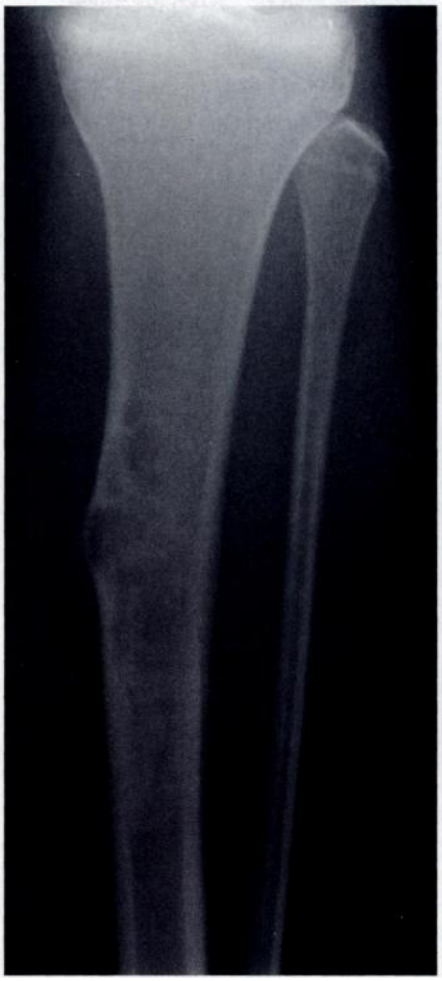

a.

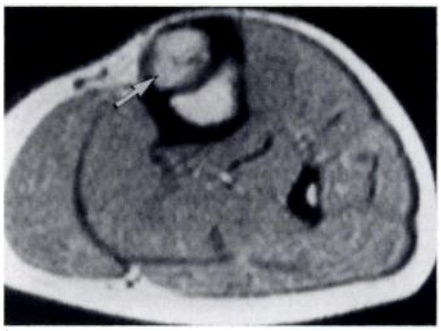

b.

Figure 13. Osteofibrous dysplasia. **(a)** Anteroposterior radiograph of the tibia shows a lobulated lesion of the proximal to midtibia shaft. The tibia is mildly bowed, and the cortex is expanded. **(b)** Axial proton-density–weighted MR image (SE 2,000/20). The intracortical location of the lesion is demonstrated (arrow).

patches of cartilage and bone scattered throughout the fat. The origin of this mineralization is debated, but it is probably the result of "modulation" or reversible shifts of mesenchymal tissues that are found beneath and within the periosteum and the overlying fibrous tissues

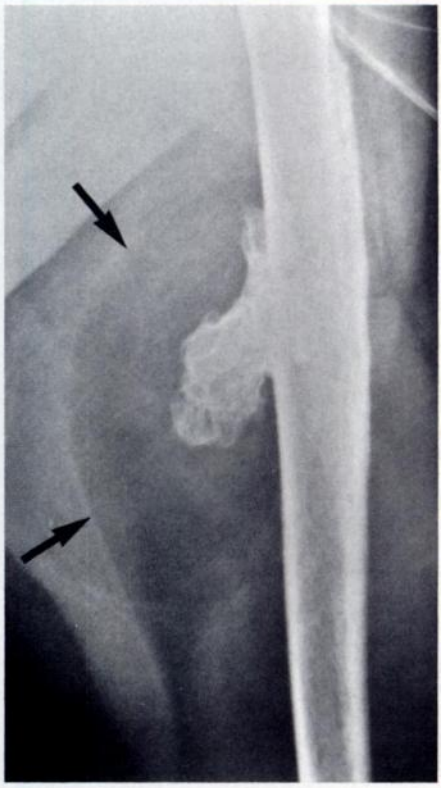

Figure 14. Parosteal lipoma. Anteroposterior radiograph of the humerus shows a dense, mature osteochondromatous lesion arising from the shaft that is surrounded by a well-defined fatty mass (arrows). (Image courtesy of Richard H. Gold, MD, Department of Radiological Sciences, University of California, Los Angeles.)

(67). The fatty component of the lesion likely does not arise from the periosteum because no fat is present in this tissue (65).

All imaging modalities will show a well-defined, homogeneous mass with the appearance of fat that is closely associated with the bone. Underlying cortical bowing or saucerization may be present (69). When a parosteal lipoma involves the extremities where the lesion is not obscured by overlying osseous structures and soft tissue, the diagnosis is usually possible with plain radiography alone because the finding of a fatty lesion adjacent to bone in association with benign bone reaction is virtually diagnostic. If cross-sectional imaging is undertaken for diagnostic or preoperative purposes, CT is preferred because MR imaging may fail to reveal subtle cortical changes (68).

VASCULAR TUMORS

Primary involvement of a bone surface by a tumor of vascular origin is rare. Preoperative diagnosis is usually challenging

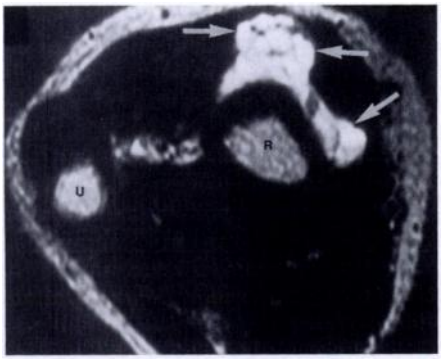

Figure 15. Parosteal hemangioma. Axial T2-weighted MR image (fast SE, 4,000/114). The lobulated, high-signal-intensity lesion (arrows) lies on the extensor surface of the radius. *R* = radius, *U* = ulna.

because the imaging appearance is often nonspecific.

Paracortical Hemangioma

Intramedullary hemangiomas are common, especially in the vertebra and the skull. In contrast, the surface hemangioma is quite unusual. Attempts have been made to differentiate between lesions that arise in the cortex and those that arise in the periosteum; however, it appears that overlap lesions occur, and this distinction is often not possible (70). The cavernous hemangioma is the most commonly encountered histologic type on the bone surface (70), but arteriovenous, venous, and granuloma type varieties may also be seen. Cure can generally be achieved with wide resection.

Radiographically, surface hemangiomas may be associated with sclerosis and cortical thickening, cortical erosion with or without adjacent sclerosis, or a permeative pattern with adjacent soft-tissue mass (70). The presence of an apparent nidus on radiographs may lead to the erroneous diagnosis of osteoid osteoma (71). Some authors have found a soft-tissue mass to be an infrequent finding (70), while others believe that a soft-tissue mass is the rule (72). The MR or CT appearance of the lesion may mimic that of a soft-tissue hemangioma (Fig 15).

Paracortical Angiosarcoma

Angiosarcoma (malignant hemangioendothelioma) of bone may be either low grade or a highly lethal tumor. The lesion may be solitary, or multifocal involvement may be present with several lesions extending either along a single bone or along a limb (73). Solitary lesions are often quite large at the time of manifestation. When multifocal, lesions are often found in both medullary and intracortical locations (Fig 16).

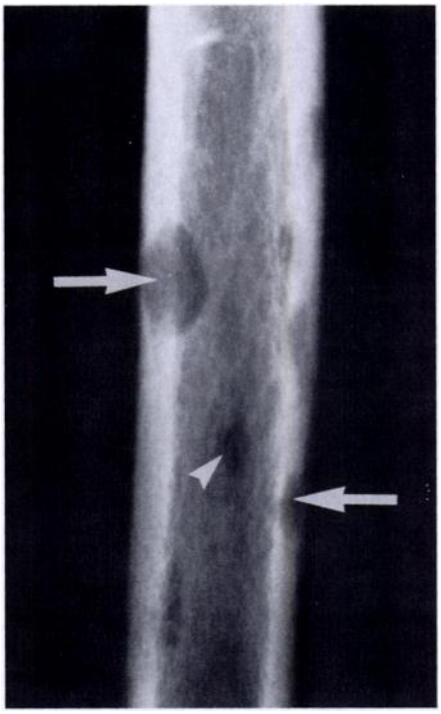

Figure 16. Angiosarcoma. Lateral radiograph of the femoral midshaft. Multiple lytic lesions are present; some appear to be cortically based (arrows), and others appear to originate in the medullary cavity (arrowhead). Confirmation of the location of any given lesion necessitates a second, perpendicular projection or cross-sectional imaging.

PAROSTEAL EWING SARCOMA

Although the cell of origin of Ewing sarcoma is debated, several studies have suggested that the tumor is derived from uncommitted skeletal mesenchyme (74,75). Conventional intramedullary Ewing sarcoma may appear radiographically as a surface lesion. Prominent surface manifestations are often present including periosteal reaction, cortical thickening, and cortical saucerization. The surface variety of Ewing sarcoma may share several features with the intramedullary lesion, including periosteal elevation and saucerization of the cortex (76,77) (Fig 2). Documentation of a surface origin is usually possible only with cross-sectional imaging. While either MR imaging or CT will demonstrate the lack of medullary involvement, the soft-tissue mass is usually better appreciated with MR. In contrast to intramedullary Ewing sarcoma, which is often diaphyseal and high grade, the periosteal lesion is more often found at the ends of long bones and seems to be associated with a less aggressive course (77).

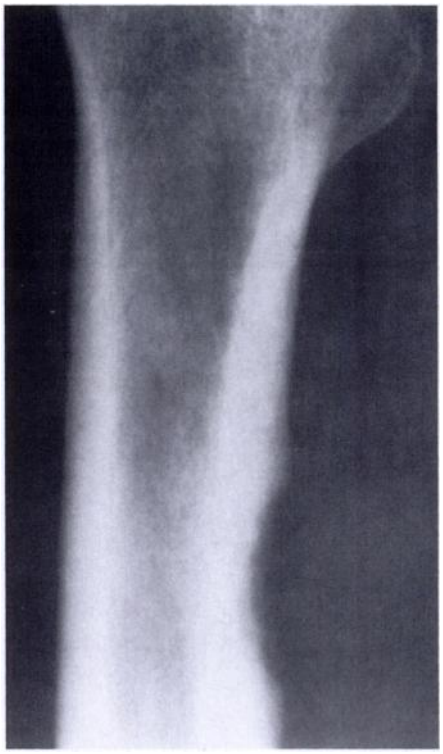

Figure 17. Parosteal metastasis (bronchogenic carcinoma). Anteroposterior radiograph of the proximal right femur shows a so-called cookie-bite lesion of the medial proximal femoral shaft.

SURFACE METASTASIS

Metastatic disease involving the surface of a bone is not uncommon. Originally thought to be specific for bronchogenic carcinoma (78), surface metastases from a variety of primary tumors have been reported including breast, kidney, pancreas, larynx, uterus leiomyosarcoma, neuroblastoma, melanoma, hepatoma, bladder, and osteosarcoma (79,80). While most of these surface metastases are referred to as "cortical," some likely originate in a subperiosteal or periosteal location (80). Whereas medullary metastases seem to have a predilection for the axial skeleton and the ends of bones, surface metastatic disease is often found in the diaphysis of long bones, especially the femur (79,80) (Fig 17).

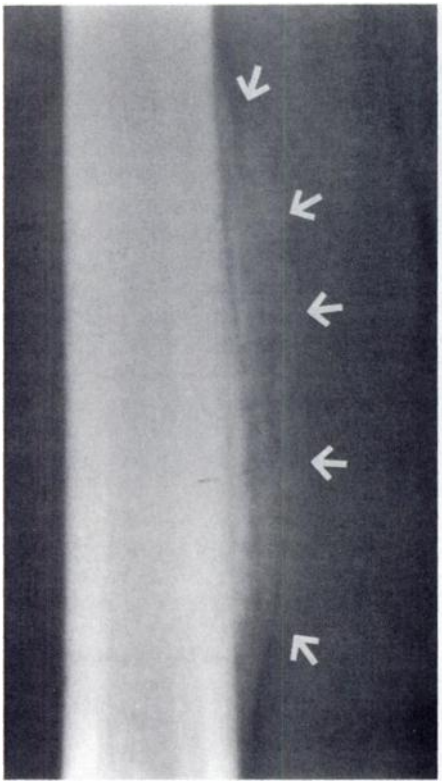

a.

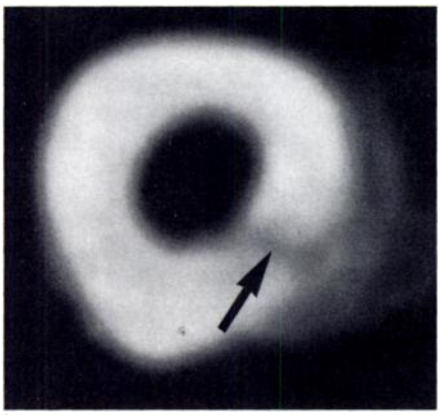

b.

Figure 18. Stress fracture. **(a)** Anteroposterior radiograph of the femur shows multilaminated, thick periosteal new bone (arrows) along the medial shaft. **(b)** CT image demonstrates the fracture line (arrow).

In one series in which cortical metastatic disease was studied, the bone lesion was the first indication of a previously undiagnosed primary malignancy in 73% of cases studied (79). This high prevalence likely reflects the study population, derived from a tumor registry that received referrals for difficult cases. Another review of radionuclide bone scans and correlative plain radiographs of 1,237 patients found a 2% prevalence of surface metastases (80). The cortical lesion was the only metastatic focus in eight of these patients.

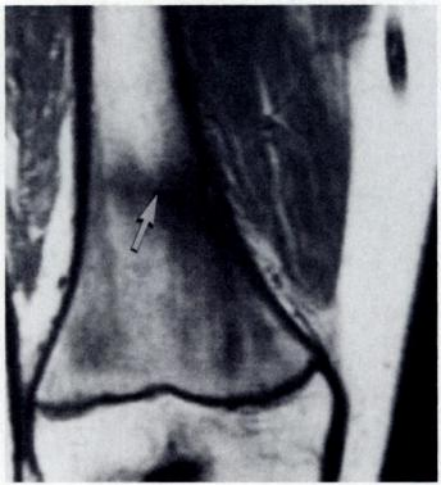

Figure 19. Stress fracture. Coronal T1-weighted MR image (SE 450/15). The fracture line is evident as a low-signal-intensity line (arrow) that is surrounded by low-signal-intensity edema.

The appearance of a surface metastasis is variable. Whereas some lesions are smoothly marginated, others have irregular, ill-defined borders. The lesion may be entirely intracortical or may extend into either the adjacent soft tissues or the medullary cavity. Because the appearance is so variable, a solitary painful surface tumor in an adult should undergo biopsy for histologic analysis.

TRAUMA

In distinct contrast to the plain radiographic identification of a fracture following a single episode of appropriate trauma, imaging manifestations of overuse conditions affecting bone may be confusing. The patient will often deny a history of substantial trauma, and, especially in childhood, a traumatic episode may be forgotten or overlooked.

The terminology used to reflect traumatic lesions to the bone surface is confusing, likely because the radiographic and histologic appearances will vary greatly depending on the time between the traumatic episode or the onset of pain and imaging or biopsy.

Stress Reaction or Stress Fracture

Although the terminology is debated, many consider isolated periostitis and/or edema to represent a stress reaction (stress response), while the presence of a fracture line indicates a true stress fracture. In reality, these two conditions represent a continuum. This arbitrary nomenclature may, however, assist in treatment planning, because more severe activity limitations may be indicated for the individual with an actual fracture line. When plain radiographs fail to reveal a fracture, the search for a cortical infraction may be accomplished with either CT (Fig 18) or MR imaging (Fig 19), although MR is probably superior if the fracture line is small and oriented in an axial plane. Thin-section imaging should be employed with either modality.

Radiographically, immature periosteal new bone may be multilaminar, but it should be uninterrupted. In the setting of an appropriate history and a reliable patient who will return for follow-up, suspected fractures can be followed clinically and radiographically to resolution. With time, the new bone will mature to become thick and unilaminar, eventually incorporating into the underlying cortex (Fig 20). If symptoms persist following cessation of the inciting activity or if maturation cannot be documented radiographically, additional imaging is warranted.

Subperiosteal Hematoma or Periostitis Ossificans

The early phase of a traumatic lesion that results in callus formation and is not associated with a fracture may represent a subperiosteal hematoma. Radiographs will reveal smooth elevation of the periosteum, and the outer cortex may be saucerized. With further maturation, periosteal ossification will be seen radiographically, and the lesion is considered a "subperiosteal ossifying hematoma" (81) or "periostitis ossificans." Histologically, the lesion may be described as a "giant cell reparative granuloma," showing giant cells, histiocytes, granulation tissue, neovascularity, reactive osteoid, and fibrosis (82). With full maturation and healing, the term "subperiosteal ossified hematoma" is appropriate. A similar condition occurring in a parosteal location may be referred to as either periostitis ossificans or myositis ossificans (Fig 21), as the exact site of origin may be impossible to ascertain pathologically.

The acute to subacute phase of this traumatic lesion involving a phalanx of the hand or foot is called "florid reactive periostitis" (83). Although a history of trauma cannot always be elicited (84), most authors believe that the lesion results from trauma induced by the surrounding soft tissues. Radiographically, florid reactive periostitis may appear as either a small, focal, oval to pedunculated

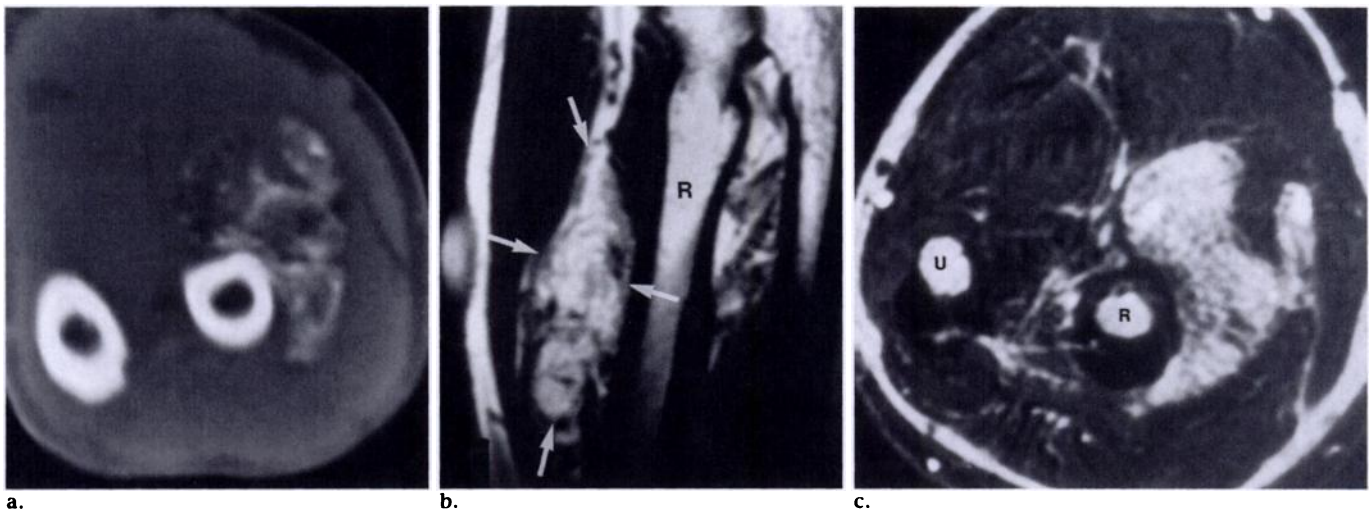

a. b. c.

Figure 21. Periostitis ossificans (juxtacortical). **(a)** CT image reveals extensive, mature ossification immediately adjacent to the cortex of the radius. **(b)** Sagittal T1-weighted MR image through the radius (SE 600/18). *R* = radius, arrows surround mass. **(c)** Axial T2-weighted MR image (SE 2,400/80). The combination of the T1- and T2-weighted image shows that the lesion contains a large amount of fat but fails to reveal the mature ossification, the key to the diagnosis. *R* = radius, *U* = ulna.

mass or as exuberant, circumferential, periosteal new bone. The underlying cortex may be mildly saucerized or may appear normal.

In the setting of an appropriate history of trauma, periostitis ossificans can be followed clinically and radiographically to confirm maturation. If cross-sectional imaging is undertaken, CT is preferred to MR imaging by virtue of its superior ability to demonstrate progressive calcification. The MR appearance may suggest a more aggressive process, leading to unwarranted intervention (85).

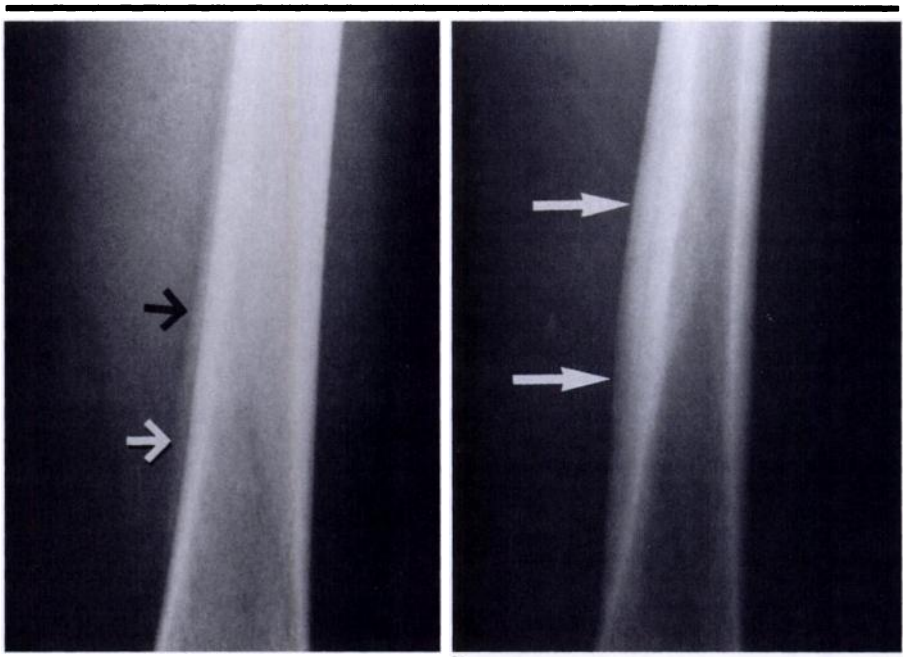

a. b.

Figure 20. Maturing traumatic periostitis.**(a)** Anteroposterior radiograph of the femoral shaft shows thick, uninterrupted, unilaminar periosteal new bone (arrows). **(b)** Anteroposterior radiograph obtained 2½ months later. The periosteal bone (arrows) has matured and is incorporated into the underlying cortex. The patient's symptoms had resolved.

Cortical Irregularity Syndrome

Cortical irregularity syndrome refers to the formation of benign periosteal new bone along the posterior, distal aspect of the femoral metaphysis, medial to the distal linea aspera. The abnormality is usually an incidental finding on radiographs obtained for an unrelated reason (57,86).

While the lesion has been commonly thought to represent a "tug" lesion at a tendinous or ligamentous attachment, this origin has been challenged. Examples of fibrous cortical defects have commonly been included in the analysis of lesions of the posterior aspect of the distal femoral shaft that have an appearance of the cortical irregularity syndrome (57). Analysis of one specimen involving the medial aspect of the distal linea aspera was found to lie in an area that lacked ligament or tendon attachments, and it was hypothesized that the cortical irregularity lesion represents an early or involuting fibrous cortical defect (86). Authors of subsequent studies, however, have concluded that the proximity of the lesion to the aponeurosis of the extensor portion of the adductor magnus muscle is sufficient to account for a traumatic origin (87,88). Resnick and Greenway (88) have further differentiated the "cystic cortical lesion" (fibrocortical lesion) from "proliferative cortical irregularity," indicating that the former arises lateral to the medial supracondylar ridge (at the site of attachment of the medial head of the gastrocnemius muscle) and the latter lies along the medial aspect of the ridge. While this differentiation may be useful in explaining the spectrum of appearances of traumatic lesions along the posterior femur, the important message is that these lesions likely share a common

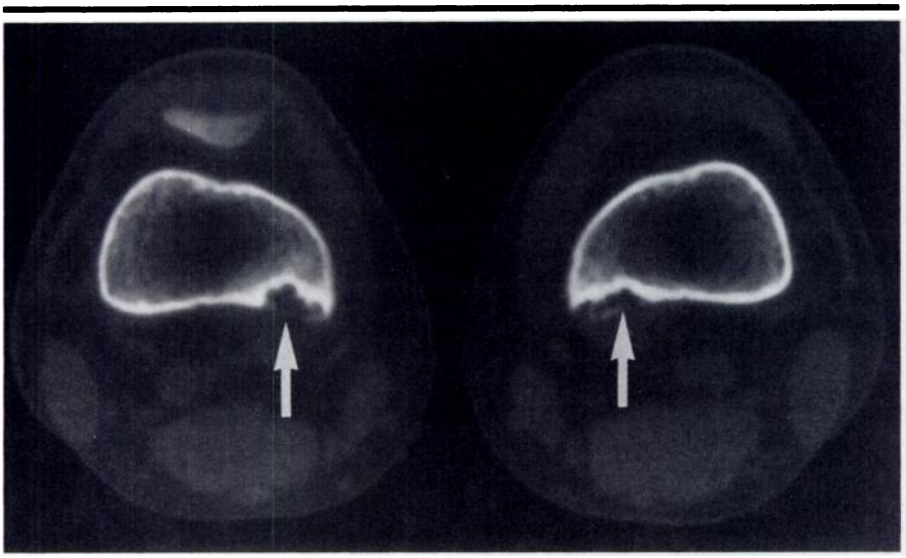

Figure 22. Cortical irregularity syndrome. CT image shows bilateral lesions of the posteromedial distal femora (arrows). The appearance, location, and bilaterality are classic for this disorder.

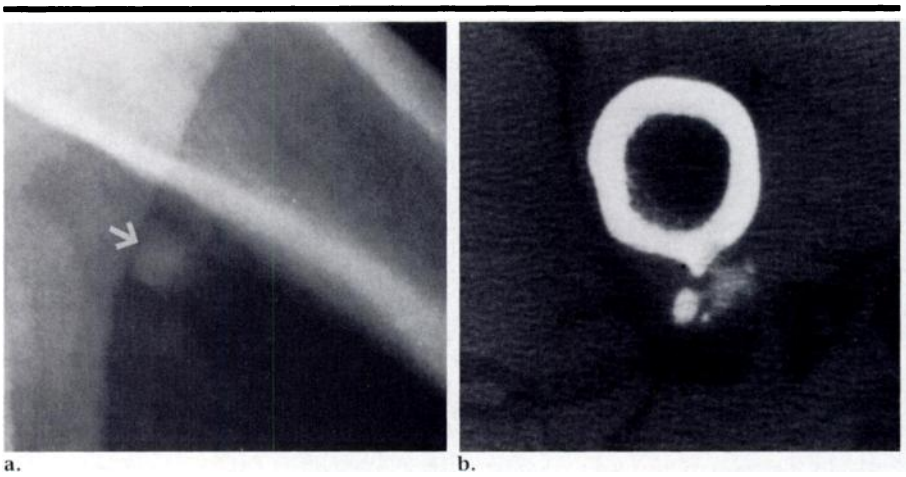

Figure 23. Tumoral-calcinosis-like lesion of the proximal linea aspera. **(a)** Lateral radiograph of the proximal femur reveals an amorphous calcification (arrow) along the posterior aspect of the proximal distal shaft. **(b)** CT image shows the origin of the lesion along the surface of the bone. Cortical erosion, commonly seen with this disorder, is lacking.

traumatic origin. The cortical irregularity syndrome has often been called a "periosteal desmoid" (89), a misnomer to be avoided. This lesion is not neoplastic as is the true desmoid tumor.

Because of its location and the fact that the lesion is found in children, the cortical irregularity syndrome (or proliferative periostitis) may be mistaken for a parosteal osteosarcoma. Confirmation of benignity is often possible by obtaining radiographs of the opposite knee, as the lesion is often bilateral (90). If radiographic findings are equivocal, a limited CT examination may demonstrate a subtle contralateral lesion (Fig 22). MR imaging plays no role in this disorder.

Calcific Tendinitis (Calcium Hydroxyapatite Deposition Disease)

When calcific tendinitis manifests in a common location such as the rotator cuff, the diagnosis is easily established on plain radiographs. When found in an unusual location and juxtacortical position, however, calcific tendinitis may appear to be a mineralized surface lesion of bone. Such a lesion occurring along the posterior aspect of the proximal thigh (linea aspera) has been termed the "tumoral-calcinosis-like lesion" (Fig 23). Although this lesion has been called calcific tendinitis or calcific periarthritis in the past (91,92), the tumoral calcinosis-like lesion is distant from the joint and lacks areas of degenerating tendon and the large numbers of inflammatory cells seen in typical calcific tendinitis (93). In addition, the pattern of fibrosis is more organized in the tumoral calcinosis-like lesion. A similar lesion may be seen along the proximal humeral shaft at the insertion of the pectoralis major (92).

In both calcific tendinitis and the tumoral calcinosis-like lesion, the calcification may be dense and well defined or amorphous. The underlying cortex may be eroded (91–93). CT is useful for demonstrating the mineralization, a feature that is easily overlooked with MR imaging. While this lesion is often mistaken for a surface osteosarcoma (93), the radiographic appearance and location at a tendinous insertion are generally diagnostic.

The patient usually presents with pain. Initial treatment consists of antiinflammatory medications, which may be followed with local steroid injection if pain relief is not achieved. Rarely, a lesion may need to be excised because of recalcitrant pain.

INFECTION

Infection of the bone surface may result from contiguous spread from the medullary cavity or adjacent soft tissues or direct inoculation during an invasive procedure. Hematogenous inoculation of the bone surface in the absence of medullary involvement is unusual.

The plain radiographic appearance of surface infection is variable. Periosteal new bone may appear relatively benign (Fig 24) or may be multilaminar and immature. A Codman triangle may be seen, indicating pus undermining and elevating the periosteum. The cortex itself may appear relatively normal, or a focal radiolucent area (intracortical abscess) may be seen.

If plain radiographs are normal and infection is suspected, MR imaging is indicated. A normal MR imaging study will essentially exclude deep infection, whereas cortical and/or periosteal edema is well displayed with MR imaging. Either MR or CT will assist in identifying an intracortical abscess; however, subperiosteal fluid collections are probably best displayed with MR imaging. Identification and documentation of abscess formation represents one of the limited uses for intravenously administered gadolinium-containing con-

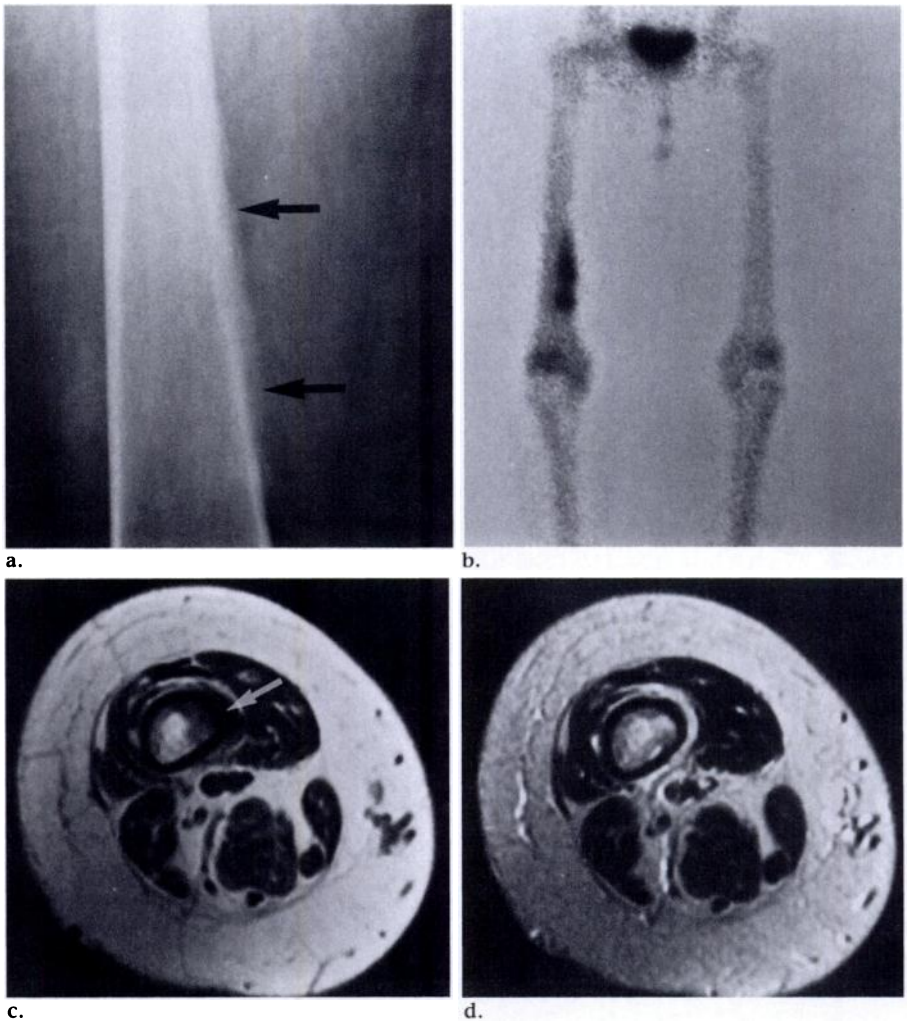

Figure 24. Parosteal osteomyelitis. **(a)** Anteroposterior radiograph demonstrates undulating but benign-appearing periosteal new bone (arrows) associated with the lateral aspect of the distal femoral shaft. **(b)** Radionuclide bone scan shows the length of the abnormality and confirmed that this was a solitary lesion. The surface origin is also evident on the bone scan. **(c)** Axial T1-weighted MR image (SE 866/17). Intermediate signal intensity is seen adjacent to the medial cortex (arrow). There is ill-defined low signal intensity in the underlying marrow, indicating edema. **(d)** Axial T2-weighted MR image (fast SE 3,500/108). The periosteal new bone and marrow edema both increase in signal intensity. A percutaneous core biopsy was performed under fluoroscopic control; the tissue sample grew *Streptococcus viridans*. The patient's sedimentation rate was mildly elevated. She denied constitutional symptoms.

trast agents in musculoskeletal MR imaging. After administration of contrast material, the cavity wall will enhance, revealing the fluid nature of the abscess (Fig 25).

The findings of edema and contrast enhancement are not specific for infection. Traumatic periostitis and some benign surface tumors (including osteoid osteoma and osteoblastoma) may have an identical appearance on MR images. Correlation with clinical and laboratory information is usually essential for establishing the diagnosis (94).

LESIONS OF UNKNOWN OR CONTROVERSIAL ORIGIN

Juxtacortical Aneurysmal Bone Cyst

Surface aneurysmal bone cysts may arise in a cortical or subperiosteal location (95). The origin of this lesion is debated, but most authors believe that the aneurysmal bone cyst represents a reactive process rather than a true neoplasm (96). This theory is supported by the fact that a history of trauma is often present (97,98). Aneurysmal bone cysts are often seen in conjunction with other intramedullary or juxtacortical lesions including nonossifying fibroma, fibrous dysplasia, chondroblastoma, giant cell reparative granuloma, simple bone cyst, giant cell tumor of bone, telangiectatic osteosarcoma, and hemangioendothelioma (99).

The imaging appearance of the juxtacortical aneurysmal bone cyst is variable, ranging from mild cortical expansion (Fig 26) to a more aggressive-appearing expansile lesion (95) (Fig 27). CT is useful in demonstrating a thin mineralized rim around the lesion and confirming the surface location along the bone. Although the surface aneurysmal bone cyst is histologically identical to the more common intramedullary lesion, the surface variety tends to recur less often (97).

Parosteal (Subperiosteal) Ganglion

The origin of the parosteal ganglion is unknown. These masses are most commonly found along the medial proximal tibia, in the region of the pes anserinus insertion. This feature has led some to speculate that tibial lesions arise from erosion or herniation of the pes bursa (100). Subperiosteal ganglia may recur following complete excision (100), perhaps because of continued stimulation from the adjacent soft tissues. Involvement of other sites including the distal shaft of the ulna, radius, and femur and the medial malleolus has been reported (100–103).

Histologically, the lining of the subperiosteal ganglion lacks a distinct cell type. Radiographically, parosteal ganglia may show no osseous abnormality or may

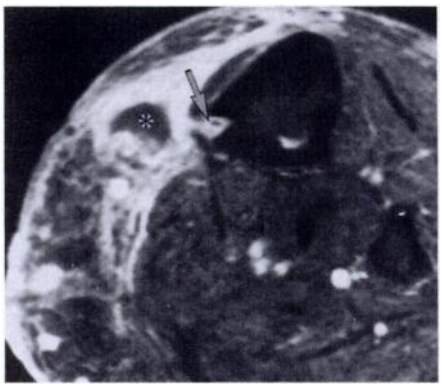

Figure 25. Cortical osteomyelitis. Contrast-enhanced T1-weighted, fat-suppressed axial MR image (SE 738/12). At presentation, the patient had cellulitis following removal of an external fixator. A well-defined focus of high signal intensity is seen within the lateral tibia cortex (arrow), adjacent to a soft-tissue abscess (*).

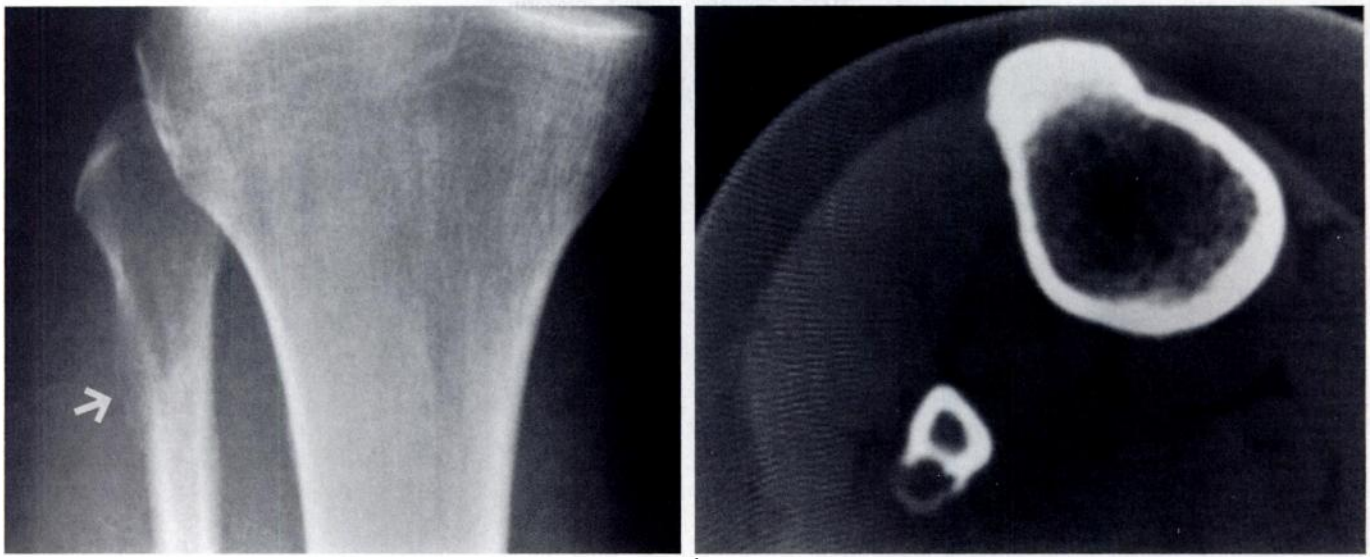

a. b.

Figure 26. Small parosteal aneurysmal bone cyst. **(a)** Anteroposterior radiograph shows unilaminar periosteal new bone (arrow) along the proximal fibular shaft. **(b)** CT image shows that the lesion is cortically based and surrounded by a thin rim of periosteal new bone.

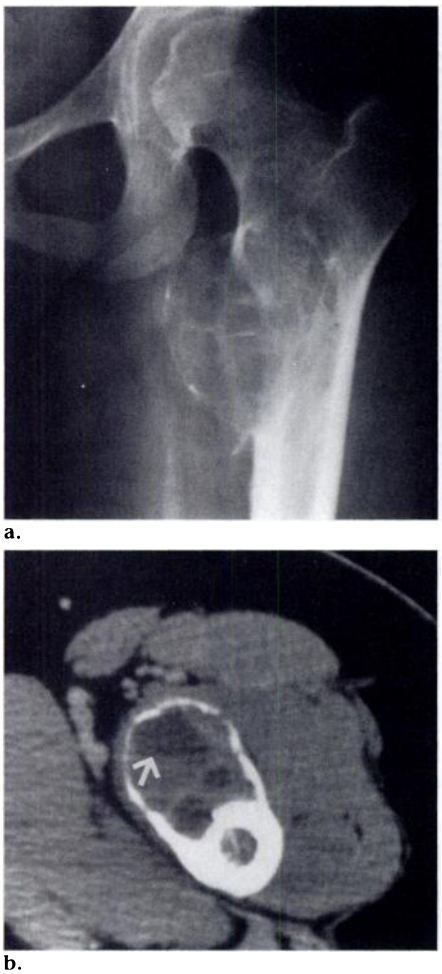

a. b.

Figure 27. Large parosteal aneurysmal bone cyst. **(a)** Anteroposterior radiograph of the right hip shows a large surface lesion arising off the anteromedial proximal femur. There is a delicate rim of bone surrounding the lesion. **(b)** Axial CT image. Note air-fluid level (arrow).

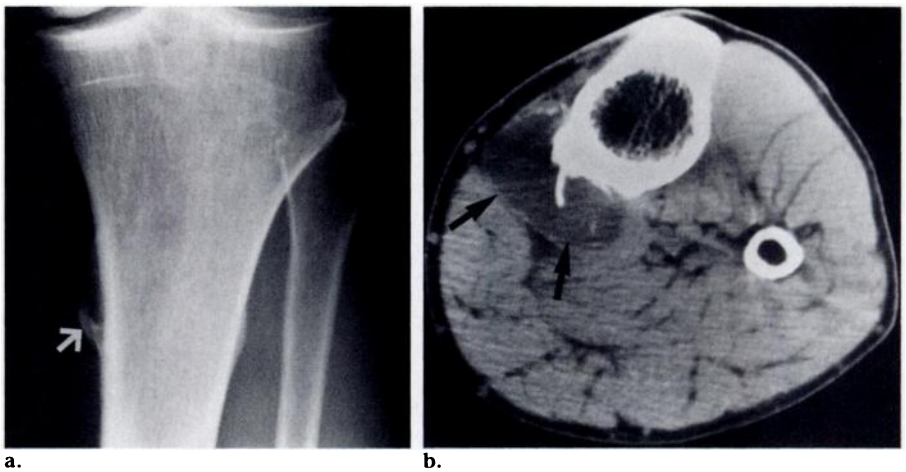

a. b.

Figure 28. Parosteal ganglion. **(a)** Anteroposterior radiograph of the proximal tibia shows mature-appearing reactive bone along the medial aspect of the proximal shaft (arrow). **(b)** CT image demonstrates the fluid-attenuation mass (arrows) that surrounds the reactive bone. (Image courtesy of Richard H. Gold, MD, Department of Radiological Sciences, University of California, Los Angeles.)

be associated with cortical erosion. The scalloping may be smooth and uniform or may be irregular, speculated, or multilobulated (100,104). Reactive bone formation may also be seen (Fig 28). Either CT or MR imaging will reveal a well-circumscribed, homogeneous lesion. CT is preferable for evaluating reactive bone formation and defining the benign character of the cortical erosion, but MR imaging may be better suited for documentation of the fluid nature of the lesion. The character of the internal fluid ranges from thin and watery to thick and mucinous. US may document that the lesion contains fluid but generally will not assist in arriving at a diagnosis.

The subperiosteal synovial cyst is closely related to the parosteal ganglion. The lining of the subperiosteal synovial cyst is composed of synovium or flattened to cuboidal cells. The latter may reflect high intracystic pressure (105).

Ribbing Disease (Multiple Diaphyseal Sclerosis)

Ribbing disease is a condition of unknown origin that is characterized by circumferential benign endosteal and periosteal new bone formation along the diaphysis of long bones (106) (Fig 29). The lower extremity is usually involved, although radiographic changes of

asymptomatic Ribbing disease of the radius has been reported in one individual who had painful lower extremity disease (107).

The patient presents with pain and/or swelling along one extremity that may be followed months to years later with similar symptoms in the opposite extremity. Although this disorder was initially described in four siblings from a single family (108), familial involvement cannot be documented in all cases.

Because the histologic characteristics of this disorder are nonspecific, Ribbing disease is a diagnosis of exclusion. In the patient with involvement of a single bone, the differential diagnosis includes stress fracture, osteoid osteoma, osteosarcoma, and osteomyelitis. The clinical history and results of laboratory evaluation are essential in arriving at the appropriate diagnosis.

CONCLUSION

Surface lesions of bone generally represent an uncommon or rare counterpart of a more common intramedullary process. As for all bone lesions, imaging evaluation should begin with plain radiography. When cross-sectional imaging is undertaken, CT is often preferable to MR imaging, because it will better depict subtle matrix mineralization or maturing periosteal new bone. Often, a diagnosis cannot be confidently made with imaging alone, and biopsy is necessary to direct patient care. Correlation with clinical information is usually essential for formulating a working diagnosis.

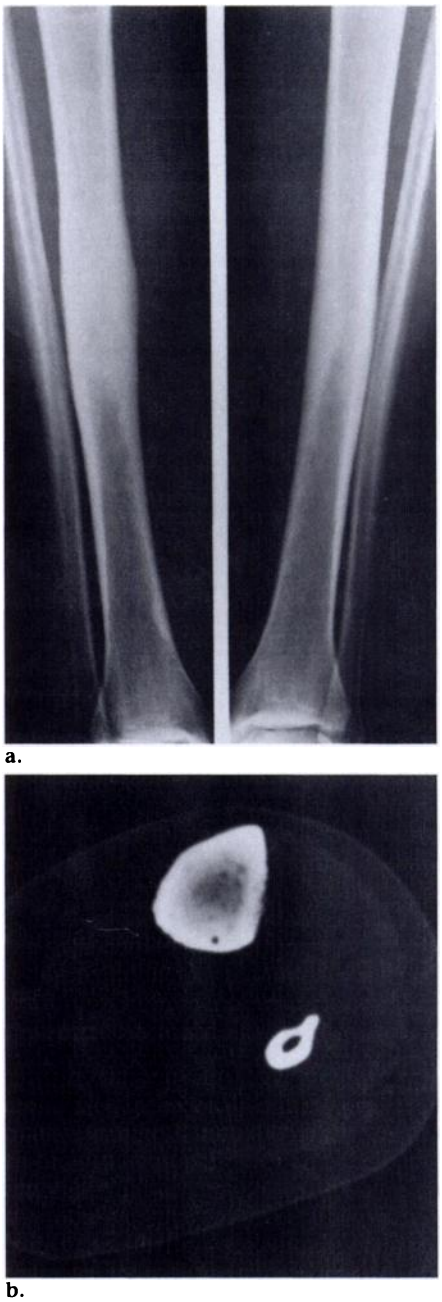

Figure 29. Ribbing disease. (**a**) Anteroposterior radiographs of the tibiae reveal marked cortical and endosteal thickening on the right, with less severe changes on the left. Only the right lower leg was symptomatic. (**b**) CT image of the left tibia shows endosteal and periosteal new bone. The medullary cavity is nearly obliterated.

References

1. Chang CH, Piatt ED, Thomas KE, Watne AL. Bone abnormalities in Gardner's syndrome. AJR 1968; 103:645–652.
2. Mirra JM, ed. Bone tumors: clinical, radiologic, and pathologic correlations. Philadelphia, Pa: Lea & Febiger, 1989; 182–183.
3. Sundaram M, Falbo S, McDonald D, Janney C. Surface osteomas of the appendicular skeleton. AJR 1996; 167:1529–1533.
4. Bertoni F, Unni KK, Beabout JW, Sim FH. Parosteal osteoma of bones other than the skull and face. Cancer 1995; 75:2466–2473.
5. O'Connell JX, Rosenthal DI, Mankin HJ, Rosenberg AE. Solitary osteoma of a long bone: a case report. J Bone Joint Surg [Am] 1993; 75:1830–1834.
6. Jaffe HL. Osteoid osteoma of bone. Radiology 1945; 45:319–334.
7. Kaye JJ, Arnold WD. Osteoid osteomas in siblings: case reports. Clin Orthop 1977; 126:273–275.
8. Kransdorf MJ, Stull MA, Gilkey FW, Moser RP Jr. Osteoid osteoma. RadioGraphics 1991; 11:671–696.
9. Glynn JJ, Lichtenstein L. Osteoid-osteoma with multicentric nidus: a report of two cases. J Bone Joint Surg [Am] 1973; 55:855–858.
10. Larsen LJ, Mall JC, Ichtertz DF. Metachronous osteoid-osteomas: report of a case. J Bone Joint Surg [Am] 1991; 73:612–614.
11. Mirra JM, ed. Bone tumors: clinical, radiologic, and pathologic correlations. Philadelphia, Pa: Lea & Febiger, 1989; 239.
12. Mirra JM, ed. Bone tumors: clinical, radiologic, and pathologic correlations. Philadelphia, Pa: Lea & Febiger, 1989; 232.
13. Schlesinger AE, Hernandez RJ. Intracapsular osteoid osteoma of the proximal femur: findings on plain film and CT. AJR 1990; 154:1241–1244.
14. Kattapuram SV, Kushner DC, Phillips WC, Rosenthal DI. Osteoid osteoma: an unusual cause of articular pain. Radiology 1983; 147:383–387.
15. Hayes CW, Conway WF, Sundaram M. Misleading aggressive MR imaging appearance of some benign musculoskeletal lesions. RadioGraphics 1992; 12:1119–1134.
16. Goldman AM, Schneider R, Pavlov H. Osteoid osteomas of the femoral neck: report of four cases evaluated with isotopic bone scanning, CT, and MR imaging. Radiology 1993; 186:227–232.
17. Assoun J, Railhac JJ, Bonnevialle P, et al. Osteoid osteomas: percutaneous resection with CT guidance. Radiology 1993; 188:541–547.
18. Lee DH, Malawer MM. Staging and treatment of primary and persistent (recurrent) osteoid osteoma: evaluation of intraoperative nuclear scanning, tetracycline fluorescence, and tomography. Clin Orthop 1992; 281:229–238.
19. Steinberg GG, Coumas JM, Breen T. Preoperative localization of osteoid osteoma: a new technique that uses CT. AJR 1990; 155:883–885.
20. Ziegler DN, Scheid DK. A method of location of an osteoid-osteoma of the femur at operation: a case report. J Bone Joint Surg [Am] 1992; 74:1549–1552.
21. Kneisl JS, Simon MA. Medical management compared with operative treatment for osteoid osteoma. J Bone Joint Surg [Am] 1992; 74:179–185.
22. Mazoyer JF, Kohler R, Bossard D. Osteoid osteoma: CT-guided percutaneous treatment. Radiology 1991; 181:269–271.
23. Atar D, Lehman WB, Grant AD. Letter: CT guided excision of osteoid osteoma. AJR 1993; 160:211.
24. Towbin R, Kaye R, Meza MP, Pollock AN, Yaw K, Moreland M. Osteoid osteoma: percutaneous excision using a CT-guided coaxial technique. AJR 1995; 164:945–949.
25. Rosenthal DI, Springfield DS, Gebhardt MC, Rosenberg AE, Mankin HJ. Osteoid osteoma: percutaneous radio-frequency ablation. Radiology 1995; 197:451–454.
26. Mirra JM, ed. Bone tumors: clinical, radiologic, and pathologic correlations. Philadelphia, Pa: Lea & Febiger, 1989; 411.
27. Kroon HM, Schurmans J. Osteoblastoma: clinical and radiologic findings in 98 new cases. Radiology 1990; 175:783–790.
28. Boriani S, Capanna R, Donati D, Levine A, Picci P, Savini R. Osteoblastoma of the spine. Clin Orthop 1992; 278:37–45.
29. O'Connell JX, Rosenthal DI, Mankin HJ, et al. A unique multifocal osteoblastoma-like tumor of the bones of a single lower extremity: a case report. J Bone Joint Surg [Am] 1993; 75:597–602.
30. Crim JR, Mirra JM, Eckardt JJ, Seeger LL. Widespread inflammatory response to osteoblastoma: the flare phenomenon. Radiology 1990; 177:835–836.
31. Schajowicz F, McGuire MH, Araujo ES, Muscolo DL, Gitelis S. Osteosarcoma arising on the surfaces of long bones. J Bone Joint Surg [Am] 1988; 70:555–564.
32. Kyraikos M. Intracortical osteosarcoma. Cancer 1980; 46:2525–2533.
33. Greenspan A, Wold L. Cortical osteosarcoma involving the medullary cavity and soft tissue: a case report. J Bone Joint Surg [Am] 1994; 76:1399–1404.
34. Okada K, Frassica FJ, Sim FH, Beabout JW, Bond JR, Unni KK. Parosteal osteosarcoma: a clinicopathological study. J Bone Joint Surg [Am] 1994; 76:366–378.
35. Kavanagh TG, Cannon SR, Pringle J, Stoker DJ, Kemp HBS. Parosteal osteosarcoma: treatment by wide resection and prosthetic replacement. J Bone Joint Surg [Br] 1990; 72:959–965.

36. Lindell MM Jr, Shirkhoda A, Raymond AK, Murray JA, Harle TS. Parosteal osteosarcoma: radiologic-pathologic correlation with emphasis on CT. AJR 1987; 148:323–328.
37. Ritts GD, Pritchard DJ, Unni KK, Beabout JW, Eckardt JJ. Periosteal osteosarcoma. Clin Orthop 1987; 219:299–307.
38. Keith A. Studies on the anatomic changes which accompany certain growth disorders of the human body. J Anat 1920; 54:101–115.
39. Dahlin DC, Coventry M. Osteogenic sarcoma: a study of six hundred cases. J Bone Joint Surg [Am] 1967; 49:101–110.
40. Anderson RL, Popowitz L, Li JK. An unusual sarcoma arising in a solitary osteochondroma. J Bone Joint Surg [Am] 1969; 51:1199–1204.
41. Lewis MM, Kenan S, Yabut SM, Norman A, Steiner G. Periosteal chondroma: a report on ten cases and review of the literature. Clin Orthop 1990; 256:185–192.
42. Morisaki Y, Takagi K, Ishii Y, Furuya T, Ishikawa M, Tanaka S. Periosteal chondroma developing in a rib at the side of a chest wall wound from a previous thoracotomy: report of a case. Surg Today 1996; 26:57–59.
43. Scarborough MT, Moreau G. Benign cartilage tumors. Orthop Clin North Am 1996; 27:583–589.
44. Kirschner SG, Pavlov H, Heller RM, Kaye JJ. Periosteal chondromas of the anterior tibial tubercle: two cases. AJR 1978; 131:1088–1089.
45. Park HR, Lee IS, Lee CJ, Park YK. Chondromyxoid fibroma of the femur: a case report with intra-cortical location. J Korean Med Sci 1995; 10:51–56.
46. Kenan S, Abdelwahab IF, Klein MJ, Lewis MM. Case report 837: juxtacortical (periosteal) chondromyxoid fibroma of the proximal tibia. Skeletal Radiol 1994; 23:237–239.
47. Mirra JM, ed. Bone tumors: clinical, radiologic, and pathologic correlations. Philadelphia, Pa: Lea & Febiger, 1989; 623.
48. Smith NC, Ellis AM, McCarthy S, McNaught P. Bizarre parosteal osteochondromatous proliferation: a review of seven cases. Aust N Z J Surg 1996; 66:694–697.
49. Meneses MF, Unni KK, Swee RG. Bizarre parosteal osteochondromatous proliferation of bone (Nora's lesion). Am J Surg Pathol 1993; 17:691–697.
50. Matsumoto K, Hukuda S, Ishizawa M, Saruhashi Y, Okabe H, Asano Y. Parosteal (juxtacortical) chondrosarcoma of the humerus associated with regional lymph node metastasis: a case report. Clin Orthop 1993; 290:168–173.
51. Schajowicz F. Juxtacortical chondrosarcoma. J Bone Joint Surg [Br] 1977; 59:473–480.
52. Bertoni F, Boriani S, Laus M, Campanacci M. Periosteal chondrosarcoma and periosteal osteosarcoma: two distinct entities. J Bone Joint Surg [Br] 1982; 64:370–376.
53. Nojima T, Unni KK, McLeod RA, Pritchard DJ. Periosteal chondroma and periosteal chondrosarcoma. Am J Surg Pathol 1985; 9:666–677.
54. Mirra JM, ed. Bone tumors: clinical, radiologic, and pathologic correlations. Philadelphia, Pa: Lea & Febiger, 1989; 1726–1727.
55. Sundaram M, McGuire MH, Schajowicz F. Soft tissue masses: histological basis for decreased signal on T2-weighted MR images. AJR 1987; 148:1247–1250.
56. Quinn SF, Erickson SJ, Dee PM, et al. MR imaging in fibromastosis: results in twenty-six patients with pathologic correlation. AJR 1990; 156:539–542.
57. Caffey J. On fibrous defects in cortical walls of growing tubular bones. Adv Pediatr 1955; 7:13–51.
58. Mirra JM, Gold RH, Rand F. Disseminated nonossifying fibromas in association with café-au-lait spots (Jaffe-Campanacci syndrome). Clin Orthop 1982; 168:192–205.
59. Crim J, Gold RH, Mirra JM, Eckardt JJ, Bassett LW. Desmoplastic fibroma of bone: radiographic analysis. Radiology 1989; 172:827–832.
60. Dong PR, Seeger LL, Eckardt JJ, Mirra JM. Case report 847: juxtacortical aggressive fibromatosis (desmoplastic fibroma) of the forearm. Skeletal Radiol 1994; 23:560–563.
61. Huvos AG, ed. Bone tumors: diagnosis, treatment, and prognosis. 2nd ed. Philadelphia, Pa: Saunders, 1991; 23.
62. Campanacci M, Laus M. Osteofibrous dysplasia of the tibia and fibula. J Bone Joint Surg [Am] 1981; 63:367–375.
63. Hazelbag HM, Taminiau AHM, Fleuren GJ, Hogendoorn PCW. Adamantinoma of the long bones. J Bone Joint Surg [Am] 1994; 76:1482–1499.
64. Moon NE, Mori H. Adamantinoma of the appendicular skeleton: updated. Clin Orthop 1986; 204:215–237.
65. Power DA. Parosteal lipoma, or congenital fatty tumor, connected with periosteum of femur. Trans Pathol Soc London 1988; 39:270–272.
66. Lidor C, Lotem M, Hallel T. Parosteal lipoma of the proximal radius: a report of five cases. J Hand Surg 1992; 17A:1095–1097.
67. Miller MD, Ragsdale BD, Sweet DE. Parosteal lipomas: a new perspective. Pathology 1992; 24:132–139.
68. Murphy MD, Johnson DL, Bhatia PS, Neff JR, Rosenthal HG, Walker CW. Parosteal lipoma: MR imaging characteristics. AJR 1994; 162:105–110.
69. Fleming RJ, Alpert M, Garcia A. Parosteal lipoma. AJR 1992; 87:1075–1084.
70. Devaney K, Vinh TN, Sweet DE. Surface-based hemangiomas of bone: a review of eleven cases. Clin Orthop 1994; 300:233–240.
71. Schajowicz F, Rebecchini AC, Bosch-Mayol G. Intracortical hemangioma simulating osteoid osteoma. J Bone Joint Surg [Br] 1979; 61:94–95.
72. Kenan S, Abdelwahab IF, Klein MJ, Lewis MM. Hemangiomas of the long tubular bone. Clin Orthop 1992; 280:256–260.
73. Huvos AG, ed. Bone tumors: diagnosis, treatment, and prognosis. 2nd ed. Philadelphia, Pa: Saunders, 1991; 581–583.
74. Hutter RV, Foote FW, Frances KC, Sherman RS. Primitive multipotential sarcoma of bone. Cancer 1966; 19:1–25.
75. Bauer F, Mirra JM, Urist MR. Bone induction by Ewing's sarcoma: transplantation into athymic nude mice. Arch Pathol Lab Med 1981; 105:322–324.
76. Mueller DL, Grant RM, Riding MD, Coopes MJ. Case report: cortical saucerization: an unusual imaging finding of Ewing sarcoma. AJR 1994; 163:401–403.
77. Shapeero LG, Vanel D, Sundaram M, et al. Periosteal Ewing sarcoma. Radiology 1994; 191:825–831.
78. Deutsch A, Resnick D. Eccentric cortical metastases to the skeleton from bronchogenic carcinoma. Radiology 1980; 137:49–52.
79. Coerkamp EG, Kroon HM. Cortical bone metastases. Radiology 1988; 169:525–528.
80. Hendrix RW, Roger LF, Davis TM Jr. Cortical bone metastases. Radiology 1991; 181:409–413.
81. Johnson MK, Lawrence JF. Metaplastic bone formation (myositis ossificans) in the soft tissues of the hand: case report. J Bone Joint Surg [Am] 1975; 57:999–1000.
82. Kenan S, Lewis MM, Abdelwahab IF, Klein M. Subperiosteal giant-cell reparative granuloma. J Bone Joint Surg [Br] 1994; 76:810–813.
83. Spjut HJ, Dorfman HD. Florid reactive periostitis of the tubular bones of the hands and feet: a benign lesion which may simulate osteosarcoma. Am J Surg Pathol 1981; 5:423–433.
84. Holmes WS, Pope TL, deLange E, Fechner RE, McDowel CL, Keats TE. Case report 413: florid reactive periostitis of the proximal phalanx of the fourth finger. Skeletal Radiol 1987; 16:163–165.
85. Karnsdorf MJ, Meis JM, Jelinek JS. Myositis ossificans: MR appearance with radiologic-pathologic correlation. AJR 1991; 157:1243–1248.
86. Brower AC, Culver JE, Keats TE. Histological nature of the cortical irregularity of the medial posterior distal femoral metaphysis in children. Radiology 1971; 99:389–392.
87. Barnes GR Jr, Gwinn JL. Distal irregularities of the femur simulating malignancy. AJR 1974; 122:180–185.
88. Resnick D, Greenway G. Distal femoral cortical defects, irregularities, and excavations: a critical review of the literature with the addition of histologic and paleopathologic data. Radiology 1982; 345–354.
89. Kimmelstiel P, Rapp I. Cortical defect due to periosteal desmoids. Bull Hosp Joint Dis 1951; 12:286–297.
90. Sontag LW, Pyle SI. The appearance and nature of cyst-like areas in the distal femoral metaphysis of children. AJR 1941; 46:185–188.
91. Hayes CW, Rosenthal DI, Plata MJ, Hudson TM. Calcific tendinitis in unusual sites associated with cortical bone erosion. AJR 1987; 149:967–970.
92. Hayes CW, Conway WF. Calcium hydroxyapatite deposition disease. RadioGraphics 1990; 10:1031–1048.
93. Seeger LL, Butler DL, Eckardt JJ, Layfield L, Adams JS. Tumoral calcinosis-like lesion of the proximal linea aspera. Skeletal Radiol 1990; 19:579–583.
94. Seeger LL, Dungan DH, Eckardt JJ, Bassett LW, Gold RH. Nonspecific findings on MR images: the importance of correlative studies and clinical information. Clin Orthop 1990; 270:306–312.
95. Schoedel K, Shankman S, Desai P. Intracortical and subperiosteal aneurysmal bone cysts: a report of three cases. Skeletal Radiol 1996; 25:455–459.
96. Fechner RE, Mills SE. Tumors of bones and joints. Washington, DC: Armed Forces Institute of Pathology, 1992; 253.
97. Capanna R, Bettelli G, Biagini R, Ruggieri P, Bertoni F, Campanacci M. Aneurysmal bone cysts of long bones. Ital J Orthop Traumatol 1985; 11:409–417.
98. Moore TE, King AR, Travis RC, Allen BC. Post-traumatic cysts and cyst-like lesions of bone. Skeletal Radiol 1989; 18:93–97.
99. Biesecker JL, Marcove RC, Huvos AG, Mike V. Aneurysmal bone cyst: a clinicopathologic study of 66 cases. Cancer 1970; 26:615–625.
100. Abdelwahab IF, Kenan S, Hermann G, Klein MJ, Lewis MM. Periosteal ganglia: CT and MR imaging features. Radiology 1993; 188:245–248.
101. Grange WF. Subperiosteal ganglion: a case report. J Bone Joint Surg [Br] 1978; 60:124–125.
102. Fisk GR. Bone concavity caused by a ganglion. J Bone Joint Surg [Br] 1949; 31:220–221.
103. McCarthy EF, Matz S, Steiner GC, Dorfman HD. Periosteal ganglion: a cause of cortical bone erosion. Skeletal Radiol 1983; 10:243–246.
104. Heyse-Moore GH, Grange WJ. Case report 82: subperiosteal ganglion. Skeletal Radiol 1979; 3:255–256.
105. Rosenthal DI, Schwartz AN, Schiller AL. Case report 179: subperiosteal synovial cyst of knee. Skeletal Radiol 1981; 7:142–145.
106. Seeger LL, Hewel KC, Yao L, et al. Ribbing disease (multiple diaphyseal sclerosis): imaging and differential diagnosis. AJR 1996; 167:689–694.
107. Paul LW. Hereditary multiple diaphyseal sclerosis (ribbing). Radiology 1953; 60:412–416.
108. Ribbing S. Hereditary, multiple, diaphyseal sclerosis. Acta Radiol 1949; 31:522–536.